UNIVERSITY OF CALIFORNIA SAN DIEGO

The Proteasome as a Drug Target in *Schistosoma mansoni*

A thesis submitted in satisfaction of the requirements for the degree of Master of Science

in

Biology

by

Steven C Wang

Committee in charge:

Professor Anthony J. O'Donoghue, Chair
Professor Conor R. Caffrey, Co-Chair
Professor Matthew D. Daugherty, Co-Chair
Professor Gen-Sheng Feng

2019

The Thesis of Steven C Wang as it is listed on UC San Diego Academic Records is approved, and it is acceptable in quality and form for publication on microfilm and electronically:

_____

_____
Co-Chair

_____
Co-Chair

_____
Chair

University of California San Diego

2019

DEDICATION

I dedicate this thesis to my loving mother, Amy Wang. Without her unconditional support and encouragement, I would not have been able to pursue my many intellectual interests.

EPIGRAPH

Specificity refers to the ability of any medicine to discriminate between its intended target and its host. Killing a cancer cell in a test tube is not a particularly difficult task: the chemical world is packed with malevolent poisons that, even in infinitesimal quantities, can dispatch a cancer cell within minutes. The trouble lies in finding a selective poison—a drug that will kill cancer without annihilating the patient. Systemic therapy without specificity is an indiscriminate bomb.

Siddhartha Mukherjee,

"The Emperor of All Maladies: A Biography of Cancer"

TABLE OF CONTENTS

LIST OF ABBREVIATIONS

Sm20S……*Schistosoma mansoni* 20S proteasome

c20S……human constitutive 20S proteasome

i20S…….human immune 20S proteasome

NTD……neglected tropical disease

PZQ.....praziquantel

AMC……...7-amido-4-methylcoumarin

AFC……7-amino-4-trifluoromethylcoumarin

Suc……..Succinyl

Ac……...Acetyl

DEAE…….Diethylaminoethyl cellulose

SDS-PAGE…….Sodium Dodecyl Sulfate-Polyacrylamide gel electrophoresis

RFU……Relative Fluorescent Units

LIST OF FIGURES

LIST OF SUPPLEMENTAL FILES

Supplementary Video 1: Three-day incubation of *S. mansoni* adult worms with MG132.

Supplementary Video 2: Three-day incubation of *S. mansoni* adult worms with DMSO control.

Supplementary Video 3: Three-day incubation of *S. mansoni* adult worms with Bortezomib.

Supplementary File 1: Total list of protein IDs with two unique peptides from mass spectrometry data.

ACKNOWLEDGEMENTS

I would like to acknowledge Professor Anthony O'Donoghue and Professor Conor Caffrey for their support and guidance as supervisors of my thesis project. Through them, I had a unique opportunity to explore science and learn a variety of tools that can be used to answer questions of my own. Brian Suzuki, Nelly El-Sakkary, and Danielle Skinner were integral to the maintenance of the *S. mansoni* life cycle, and without them, this work would not be possible. Betsaida Bibo-Verdugo generated most of the preliminary data that lead to this project, and Jehad Almaliti and Dr. William Gerwick generously provided the small molecule chemistries.

I would also like to acknowledge several individuals who have inspired my intellectual interests. Chris Lietz not only taught me how to apply mass spectrometry to study proteins and peptides, but also introduced me to the principles behind the operation of mass spectrometers. Andrew Nelson showed me how small molecules can be made with rudimentary glassware, and a bit of retrosynthetic insight. He taught me never to lose sight of my goals, no matter how repetitive lab work can be. Zhenze Jiang, whom I have worked side by side now for close to two years, was a close friend, both in and out of the laboratory.

Chapter 2, in full, is a reprint of the material as it appears in The Proteasome as a Drug Target in the Metazoan Pathogen, *Schistosoma mansoni*. Bibo-Verdugo, Betsaida; Wang, Steven; Almaliti, Jehad; Ta, Anh; Jiang, Zhenze; Wong, Derek; Lietz, Christopher; Suzuki, Brian; El-Sakkary, Nelly; Hook, Vivian; Salvesen, Guy; Gerwick, William; Caffrey, Conor; O'Donoghue, Anthony; ACS Infectious Diseases, 2019. The thesis author was the joint first author of this paper.

Chapter 3, in full, is a reprint of the material as it appears in The Proteasome as a Drug Target in the Metazoan Pathogen, *Schistosoma mansoni*. Bibo-Verdugo, Betsaida; Wang,

Steven; Almaliti, Jehad; Ta, Anh; Jiang, Zhenze; Wong, Derek; Lietz, Christopher; Suzuki, Brian; El-Sakkary, Nelly; Hook, Vivian; Salvesen, Guy; Gerwick, William; Caffrey, Conor; O'Donoghue, Anthony; ACS Infectious Diseases, 2019. The thesis author was the joint first author of this paper.

Chapter 4, in full, is a reprint of the material as it appears in The Proteasome as a Drug Target in the Metazoan Pathogen, *Schistosoma mansoni*. Bibo-Verdugo, Betsaida; Wang, Steven; Almaliti, Jehad; Ta, Anh; Jiang, Zhenze; Wong, Derek; Lietz, Christopher; Suzuki, Brian; El-Sakkary, Nelly; Hook, Vivian; Salvesen, Guy; Gerwick, William; Caffrey, Conor; O'Donoghue, Anthony; ACS Infectious Diseases, 2019. The thesis author was the joint first author of this paper.

Chapter 5, in full, is a reprint of the material as it appears in The Proteasome as a Drug Target in the Metazoan Pathogen, *Schistosoma mansoni*. Bibo-Verdugo, Betsaida; Wang, Steven; Almaliti, Jehad; Ta, Anh; Jiang, Zhenze; Wong, Derek; Lietz, Christopher; Suzuki, Brian; El-Sakkary, Nelly; Hook, Vivian; Salvesen, Guy; Gerwick, William; Caffrey, Conor; O'Donoghue, Anthony; ACS Infectious Diseases, 2019. The thesis author was the joint first author of this paper.

The research reported here was supported by R21AI133393 to Dr. Anthony O'Donoghue and R21AI126296 to Dr. Conor Caffrey. *S. mansoni*-infected hamsters were in part provided by the NIH-NIAID Schistosomiasis Resource Center for distribution through BEI Resources, NIH-NIAID Contract HHSN272201700014I. Co-contributors of the research Zhenze Jiang is supported by the UCSD Chancellor's Research Excellence Scholarship, Christopher Lietz by NIH T32MH019934, and Jehad Almaliti by the University of Jordan and the Scientific Research Support Fund.

VITA

2013-2017 Bachelor of Science, Biochemistry and Cell Biology, University of California San Diego

Bachelor of Arts, Psychology, University of California San Diego

Bachelor of Science, Marine Biology, University of California San Diego

2018-2019 Master of Science, Biology, University of California San Diego

PUBLICATIONS

Monti L, Wang SC, Oukoloff K, Smith AB, Brunden KR, Caffrey C, Ballatore C. (2018) Brain-penetrant, triazolopyrimidine and phenylpyrimidine microtubule-stabilizers as potential leads to treat human African trypanosomiasis. ChemMedChem. 2018 Sep 6;13(17):1751-1754. https://doi.org/10.1002/cmdc.201800404

Lapek JD Jr, Jiang Z, Wozniak JM, Arutyunova E, Wang SC, Lemieux MJ, Gonzalez DJ, O'Donoghue AJ. (2019) Quantitative Multiplex Substrate Profiling of Peptidases by Mass Spectrometry. Molecular & Cellular Proteomics. 2019 May;18(5):968-981. https://doi.org/10.1074/mcp.TIR118.001099

ABSTRACT OF THE THESIS

The Proteasome as a Drug Target in *Schistosoma mansoni*

by

Steven C Wang

Master of Science in Biology

University of California San Diego, 2019

Professor Anthony J. O'Donoghue, Chair
Professor Conor R. Caffrey, Co-Chair
Professor Matthew D. Daugherty, Co-Chair

Proteases are fundamental to successful parasitism, including for the schistosome flatworm parasite, which causes the disease schistosomiasis in 200 million people worldwide. One protease complex, the proteasome, is receiving much attention as a potential drug target for treatment of a variety of infectious parasitic diseases but has been relatively understudied in the schistosome.

Adult *Schistosoma mansoni* was incubated in the presence of 1 μM of the commercial proteasome inhibitors bortezomib, carfilzomib and MG132. After 24 h, bortezomib and carfilzomib decreased worm motility by more than 85% and inhibited endogenous proteasome activity by >75% relative to DMSO controls. The clear association between the engagement of the proteasome target, and the phenotypic and biochemical effects recorded, encouraged the two-step chromatographic enrichment of the *S. mansoni* proteasome (Sm20S). Proteomic analysis of Sm20S identified 14 subunits each with an ortholog in the constitutive human proteasome. Activity assays with standard fluorescent substrates for the β1, β2 and β5 proteasome subunits revealed that Sm20S contains caspase-type (β1), trypsin-type (β2) and chymotrypsin-type (β5) activities. Sm20S was screened with 11 peptide epoxyketone inhibitors derived from the marine natural product, carmaphycin B. Analog 17 exhibited preferential inhibition of the Sm20S β2 and β5 subunits over that of c20S and i20S. Furthermore, 1 μM of 17 decreased both worm motility and endogenous Sm20S activity by more than 90% after 24 h. We provide direct evidence of the proteasome's importance to schistosome viability and identify a lead for which future studies will aim to improve the potency, selectivity and safety.

INTRODUCTION

Schistosomiasis is a chronic parasitic infection caused by three main species of trematode blood flukes: *Schistosoma mansoni*, *Schistosoma haematobium*, and *Schistosoma japonicum*[1–5]. These worms undergo a complex multi-stage life cycle. In brief, adult schistosome worms form male and female pairs in the veins of the human host, where they reproduce and lay fertilized eggs. These eggs are either trapped within the human host tissue, where they can cause inflammation, or excreted into the environment through the feces. Eggs will then hatch into miracidia, infect a suitable intermediate snail host, and undergo asexual reproduction. Next, the cercariae stage, which are released into freshwater from the snail host, infect the definitive human host by penetrating through the skin upon contact, and eventually mature into adult worms, thus completing the life cycle.

Adult schistosomes are sexually dimorphic. In general, male worms are slightly shorter and wider than their female counterparts, while female worms are slender and longer in length: male *S. mansoni* worms measure 9-12 mm in length and females measure 12-16 mm in length, though these sizes differ with the other species of schistosomes[4]. When paired, female worms reside within a groove running down the center length of the male worm. This pairing leads to gene expression changes in the female worm and is requisite for their complete physical and reproductive development[6].

Once mature, the female worms can produce over three hundred eggs a day[4]. The egg morphology is different for each of the three disease causing schistosomes, and is exploited as a clinical diagnostic tool. In *S. mansoni*, eggs are elongated and roughly 140 μm in length[4]. They feature an offset spine at the posterior end pointing to the side[4]. Once *S. mansoni* eggs are released, they travel through the intestinal tract and are excreted from the human host along with feces.

When eggs contact a freshwater source, they hatch into miracidia. During this stage, the miracidia must find a suitable snail host within twelve hours of hatching, or they deplete their energy stores and die[4]. *S. mansoni* miracidia infect snails of the *Biomphalaria* species, which they seek out with a combination of positive phototaxis and chemotaxis[4]. Once physical contact is made, the miracidia burrow through the soft tissue of the snail. They undergo a developmental change into the primary sporocyst stage, and asexually reproduce within the snail host[4]. After several weeks of development, the primary sporocyst stage transforms first into numerous secondary sporocysts, then into the cercariae stage. The mature cercariae stage leave the intermediate snail host into the surrounding environment.

S. mansoni in the cercariae stage swim through freshwater in search of a human host to continue development into the adult form. Cercaria are approximately 500 μm in length, with a main body attached to a bifurcated tail that propels them through water[4]. They locate their host by homing in on chemical attractants, particularly those present in human skin such as linoleic acid and arginine[7]. Once cercaria encounter human skin, they secrete various proteolytic enzymes that assist penetration of the epidermis layer[8]. During this process, the tail end of the cercaria detaches and only the main body enters the human host[4]. Once inside, cercaria develop into the juvenile schistosomulum stage.

Schistosomulum undergo a developmental change while they migrate through the human host. Starting from the skin, schistosomulum enter the blood vasculature and pass through the lungs[9]. During this time, the schistosomulum start to elongate and become more worm-like in appearance[4]. Eventually, in the case of *S. mansoni*, the schistosomulum make their way to the liver, where they finish development into adult male and female schistosome worms[9]. These worms pair and then migrate to their final destination in the mesenteric veins that drain from the

small intestine[4]. The adult worm life span has been estimated to be between 5 and 10 years; however, cases of schistosomiasis lasting up to 38 years have been reported[10–12].

The WHO estimates that over 200 million people are at risk of this disease and may require preventative treatment. The geographic distribution of schistosomiasis is partially driven by the natural habitats of the intermediate snail host. At risk populations in the tropical and sub-tropical regions are often those in poverty without access to clean water and sanitation. Schistosomiasis can cause death, but as a chronic infection, it more often than decreases productivity and leads to impaired development in children. Populations affected by schistosomiasis are then locked in a cycle of poverty. As a result of its significant socioeconomic cost, schistosomiasis is classified as a neglected tropical disease (NTD), second only to malaria in terms of impact[13].

Upon infection, early clinical manifestations of schistosomiasis include raised lesions at the side of cercariae penetration. Naïve patients may often develop a skin reaction, or a rash shortly after infection[14]. Individuals with re-infection of schistosomiasis can develop Katayama fever, which is an acute form of schistosomiasis mediated by the immune response. Symptoms during acute schistosomiasis can include high fever, fatigue, myalgia, and abdominal tenderness[15,16]. Even though mortality rates can be as high as 25%, most patients do not develop Katayama fever[15]. Chronic schistosomiasis is most often associated with the local host inflammatory response to schistosome eggs. When eggs become trapped in host tissue, they induce an immune response that leads to the formation of granulomas. The human immune system is eventually able to destroy these eggs but results in fibrosis at the site of clearance. Eggs that are trapped in the gut lead to a variety of gastrointestinal diseases, eggs trapped in the liver lead to liver fibrosis, and eggs trapped in the lungs cause pulmonary issues[1,5,15,16]. Finally, in neuroschistosomiasis, aberrantly migrating

worm pairs deposit eggs in the brain or spinal cord, causing granulomas in the central nervous system[14].

The currently approved treatment for schistosomiasis is praziquantel (PZQ). This drug, a pyrazinoisoquinoline derivative, is effective against all three disease causing species of schistosomes, but only against the adult worm life stage. Re-infection can often occur when juvenile stage worms survive the standard treatment regimen. The precise mechanism of action of praziquantel remains unknown, but it is believed to target parasite calcium ion channels[17,18]. Although experimental studies in the lab have reported praziquantel resistance, praziquantel has been used successfully in patients that have undergone multiple treatment courses over a span of more than 10 years[14]. However, lingering concerns remain given that praziquantel is the only treatment method used. It is therefore important to develop drugs that can not only effectively treat all life cycle stages of schistosomiasis, but also act on an alternative mechanism of action.

Proteasome inhibitors are a class of chemical compounds that have recently shown promise against a variety of pathogenic agents[19]. These chemistries target the proteasome complex, a large multi-subunit protein complex that is responsible for regulating protein turnover in all eukaryotic cells as part of the ubiquitin proteasome pathway[20]. A 20S proteasome core and 19S proteasome cap comprise the 26S proteasome complex, with the naming nomenclature derived from the sedimentation coefficient of each respective subunits. By mass the 20S core is approximately 750 kDa, while the 19S cap is approximately 700 kDa[21]. The subunits that make up the 19S cap have many functions such as ATP hydrolysis, ubiquitin binding, and de-ubiquitination. This cap, when bound to the barrel shaped 20S core, serves to feed ubiquitinated proteins into the catalytic center of the 20S core for proteolytic degradation. Because the channel in the 20S core is rather narrow, the 19S cap also helps unfold targeted proteins through an unknown mechanism[21]. The 20S

proteasome core itself is made up of alpha and beta subunits. These subunits are stacked on top of one another, forming a barrel like structure, with the two rings of seven alpha subunits forming the entrance of the barrel and two rings of seven beta subunits comprising the middle. Out of a total of fourteen subunits, the catalytic subunits of the 20S proteasome core are the β1, β2, and β5 subunits. These three subunits each have a different substrate specificity, which are caspase-like, trypsin, and chymotrypsin respectively. Within each subunit, an active site threonine residue is responsible for catalysis.

In response to the expression of interferon gamma (IFN-γ), alternative catalytic subunits are expressed and incorporated into the 20S proteasome complex. This results in a different complex called the immunoproteasome, with its catalytic subunits termed β1i, β2i, and β5i. The immunoproteasome has more specialized functions in generating MHC class I molecules for antigen presentation, as well as other immune system related functions[22]. Gene knockouts of the immunoproteasome catalytic subunits in mice lead to defective antigen processing[23–25]. Furthermore, the immunoproteasome has been shown to have distinct substrate specificities than the constitutive 20S proteasome[22]. Here, we distinguish between the constitutive proteasome and immunoproteasome by terming them c20S and i20S respectively. Finally, it has recently been shown that the thymus expresses a different catalytic subunit, the β5t, forming the thymoproteasome[21].

Known proteasome inhibitors either act as active site inhibitors and bind to some, if not all of the catalytic β subunits, or are allosteric inhibitors. The clinically approved proteasome inhibitors bortezomib (Velcade®) and carfilzomib (Kyprolis®) are used to treat multiple myeloma. These are both small molecule chemistries based on a peptide backbone, each containing a chemical warhead that covalently reacts with the active site threonine residue of the proteasome

catalytic subunits. Once the active site is blocked, the proteasome is no longer able to function in proteolysis. While both bortezomib and carfilzomib were designed to target the human 20S proteasome, because the proteasomal degradation pathway is well conserved across eukaryotes, they are also able to broadly act against many infectious agents, such as the parasites *Trypanosoma brucei* and *Plasmodium falciparum*[26,27]. Recent reports have demonstrated that it is possible to design active site inhibitors against the *P. falciparum* 20S proteasome with greater than 300 fold selectivity compared to the human 20S proteasome[28]. On the other hand, a large scale medicinal chemistry campaign has led to the development of non-competitive inhibitors that target the non-catalytic β4 subunit of the 20S proteasome in kinetoplastid parasites *Trypanosoma cruzi*, *Trypanosoma brucei*, and *Leishmania donovani*[29]. These inhibitors have over eight hundred fold selectivity and oral in vivo efficacy[29]. These developments have shown that there is still a relatively unexplored therapeutic space for developing proteasome inhibitors.

In this study, we report identifying the *Schistosoma mansoni* 20S proteasome (Sm20S) as a potential druggable target in treating schistosomiasis. We show that proteasome inhibitors can kill adult *S. mansoni* worms in vitro. We then characterize the Sm20S proteasome by enriching the enzyme complex from *S. mansoni* using a two-step column chromatography procedure. We focus on a small chemical library of carmaphycin analogs generously shared by Dr. Gerwick of the Scripps Institute of Oceanography. Carmaphycin B is a proteasome inhibitor and marine natural product originally isolated and characterized from cyanobacterium found in Curacao[30]. They are peptide like inhibitors consisting of a three amino acid backbone, and an epoxyketone chemical warhead that reacts with the active site threonine residue in the β1, β2, and β5 subunits. Our group has previously shown that the carmaphycin analogs are potent against *Plasmodium falciparum*[28] and thus these analogs were readily available to us. We show here that one analog

preferentially targets Sm20S over the human proteasome and demonstrated decreased mammalian cytotoxicity.

MATERIALS AND METHODS

Maintenance of *S. mansoni*

S. mansoni was maintained in male Golden Syrian hamsters and *Biomphalaria glabrata* (NMRI isolate) vector snails. Hamsters were infected at four weeks of age with 600-800 *S. mansoni* cercariae. At seven weeks post-infection, animals were euthanized by a lethal injection of sodium pentobarbital solution (Fatal-Plus; Vortech Pharmaceuticals Ltd) and adult worms harvested by reverse perfusion of the hepatic portal system[31–34]. Maintenance and handling of small vertebrate animals were carried out in accordance with a protocol approved by the Institutional Animal Care and Use Committee (IACUC) of the University of California San Diego. UCSD-IACUC derives its authority for these activities from the United States Public Health Service (PHS) Policy on Humane Care and Use of Laboratory Animals, and the Animal Welfare Act and Regulations (AWAR).

Quantitative phenotypic effects of proteasome inhibitors on adult *S. mansoni in vitro.*

After perfusion, parasites were washed extensively in Basch medium 169 [34,35].Worms were distributed into 24w plates at five-six adult pairs per well and allowed to acclimatize overnight at 37 ºC and 5% CO_2 in 1 ml Basch medium containing 4% heat-inactivated FBS. The next morning, a final concentration of 1 µM of proteasome inhibitor (dissolved in DMSO) was added and the volume made up to 2 ml (final DMSO concentration was 0.05%). After 1, 6 and 24 h, worm motility was measured using WormAssay[36–38]. WormAssay comprises a commodity digital movie camera connected to an Apple Mac computer that operates an open source software application to automatically process multiple wells in 6-, 12- or 24-well plate geometries. Using the "Consensus Voting Luminance Difference" option, the application detects the aggregate changes in the occupation and vacancy of pixels between frames that are due to worm movement. Parasites were

also observed using an inverted microscope (Zeiss AxioVert A1, 1.25X objective) at the same time points and up to 72 h, and changes in motility, shape, color and pairing status recorded using a constrained nomenclature [34,37,39,40].

Evaluation of caspase activation in worms exposed to proteasome inhibitors.

After recording the phenotypic responses in the presence of proteasome inhibitors, worms were transferred to 1.5 mL tubes and washed with 0.5 ml of ice-cold PBS every 30 min for 2 h. Worms were allowed to settle and subsequently homogenized in 130 µL of 40 mM PIPES, 20% sucrose, 200 mM NaCl, 2% CHAPS, 2 mM EDTA, pH 7.2, using a pestle connected to a hand-held motor. The lysate was centrifuged for 10 min at 15,000 ×*g* and 4 °C, and the supernatant was recovered for analysis. The protein concentration was quantified using the Pierce BCA kit (Thermo Scientific). Prior to assaying for caspase activity, the supernatant was pre-incubated at 37 °C for 1 h in the above buffer containing 10 mM DTT. Likewise, 200 µM of the caspase substrate, Ac-Asp-Glu-Val-Asp-7-amino-4-trifluoromethylcoumarin (Ac-DEVD-AFC; CPC Scientific) was pre-incubated at 37 °C for 10 min in the same buffer containing 10 mM DTT. Equal volumes of both the supernatant and substrate were then mixed in white-walled 96-well flat-bottomed plates and activity was measured using a CLARIOstar monochromator microplate reader (BMG Labtech) at excitation and emission wavelengths of 400 nm and 505 nm, respectively. Activity was quantified as relative fluorescence units (RFU) min^{-1} μg^{-1} protein.

Inhibition of proteasome activity in *S. mansoni* extracts.

To prepare *S. mansoni* lysates, mixed-sex adult worms were homogenized using a pestle connected to a handheld motor in 1.5-ml tubes containing 100 mM Tris-HCl, 100 µM E-64, pH 7.5. Lysates were then centrifuged for 15 min at 15,000 ×g and 4 °C. The upper lipid layer was discarded and the protein concentration of the remaining supernatant was quantified using the

Pierce BCA kit. Supernatants were incubated with inhibitors for 1 h at room temperature and activity was assayed in 50 µl total volume reactions containing 7.5 µg of protein and 25 µM of the substrate, Succinyl-Leu-Leu-Val-Tyr-7-amido-4-methyl coumarin (Suc-LLVY-AMC), in 20 mM Tris-HCl, 0.02% SDS, pH 7.5, in black, round-bottomed 96w plates. The final concentration of inhibitors used was 10 µM E-64 and 1 µM for the proteasome inhibitors. Controls contained 0.0001% DMSO. The release of the AMC fluorophore was monitored at 24°C in a Synergy HTX multi-mode reader (BioTek Instruments, Winooski, VT) with excitation and emission wavelengths set to 340 nm and 460 nm, respectively. Activity was quantified as RFU min^{-1} μg^{-1} protein and normalized to the DMSO control reactions.

Evaluation of proteasome inhibition in worms exposed to proteasome inhibitors.

After evaluation of the phenotypic responses in the presence of proteasome inhibitors, worms were transferred to 1.5 ml tubes and washed with 0.5 ml of ice-cold PBS every 30 min for 2 h. Protein lysates were prepared from homogenized worms as described above and assays were performed with 25 µM Suc-LLVY-AMC in 20 mM Tris–HCl, 0.02% SDS, pH 7.5. Activity was expressed as RFU min^{-1} μg^{-1} and normalized to the DMSO control reactions.

Enrichment of the *S. mansoni* proteasome.

The starting material for enrichment of the *S. mansoni* proteasome (Sm20S) was approximately 500 adult worm pairs that had been extensively washed in PBS and frozen at -80 °C. Worms were homogenized using a pestle connected to a motor in 1.5-ml tubes in ice cold 100 mM Tris-HCl, 100 µM E-64, pH 7.5. Lysates were centrifuged for 15 min at 10,000 ×*g* and 4 °C, and the supernatant subjected to two ammonium sulfate precipitation steps, each for 30 min on ice, at 30 and 60% saturation, respectively. After centrifugation for 15 min at 10,000 ×g and 4 °C, the supernatant was discarded and the precipitated proteins were re-suspended in 5 mL of ice cold 100

mM Tris-HCl, pH 7.5. Protein was concentrated and buffer exchange into 20 mM Tris-HCl, 10% glycerol, 0.125 M NaCl, pH 7.5 using a 100 kDa centrifugal filter unit (Amicon). Approximately 5 mg of soluble protein was loaded onto a Superose 6 10/300 gel filtration column under the control of an ÄKTA Pure instrument (GE Healthcare Life Sciences). Protein was eluted using 20 mM Tris-HCl, 10% glycerol, 0.125 M NaCl, pH 7.5. Fractions of 0.5 mL were collected, and assayed for proteasome activity with 25 μM Suc-LLVY-AMC in assay buffer (20 mM Tris, 0.02% SDS, pH 7.5). The AMC fluorophore release was monitored at 24°C with excitation and emission wavelengths of 340 nm and 460 nm, respectively, using a Synergy HTX multi-mode reader (BioTek Instruments).

Fractions containing proteasome activity were pooled and loaded onto a 5 ml anion exchange HiTrap DEAE FF column. Protein was eluted using 20 mM Tris-HCl, 10% glycerol, pH 7.5, and a linear gradient from 0.125 to 0.6 M NaCl. Fractions (1.5 ml) were collected and assayed with Suc-LLVY-AMC. Fractions containing proteasome activity were pooled and an aliquot was denatured and loaded into a 4-12% Bis-Tris Plus gel (Thermo Scientific) next to 70-130 ng of the human constitutive proteasome, c20S (Boston Biochem). The gel was stained using the Pierce silver stain kit (Thermo Scientific) and the concentration of Sm20S was estimated by comparing band density with the highly purified human c20S proteasome using Image J software.

Gel slice excision and proteomics.

Silver stained gel bands were excised with a clean scalpel, diced into 1 mm cubes and placed into 0.6 mL tubes (Axygen). An in-gel digestion was performed as described by Shevchenko and colleagues[41]. Following digestion and extraction, the peptides were desalted with C18 LTS tips (Rainin) and dried in a vacuum centrifuge. Peptides were resuspended in 12 μL 0.1% TFA and 5 μL was analyzed on a Q Exactive Mass Spectrometer (Thermo Scientific). Peptides

were separated by reverse phase chromatography on an UltiMate 3000 HPLC system (Thermo Scientific) equipped with an in-house packed C18 column (1.7 µm bead size, 75 µm × 25 cm, heated to 65 ºC) at a flow rate of 300 nL/min over a 76-minute linear gradient from 5% Solvent A to 25% Solvent B, where solvent A and B correspond to 0.1% formic acid in water and 0.1% formic acid in acetonitrile, respectively. Survey scans were recorded at a resolution of 35,000 at 200 m/z over a range of 350-1500 m/z with the automatic gain control (AGC) at 1×10^6 and a maxIT of 300 ms. MS/MS was performed in data-dependent acquisition mode with higher-energy collision dissociation (HCD) fragmentation (28 normalized collision energy) on the 20 most intense precursor ions at a resolution of 17,500 at 200 m/z with the AGC at 5×10^6 and a maxIT of 50 ms.

Data analysis was performed using the PEAKS 8.5 software (Bioinformatics Solutions Inc.). RAW files were searched against the *S. mansoni* (Puerto Rican isolate; UP000008854) reference proteome from UniProt that contains 11,723 entries with the following settings: 15 ppm precursor mass tolerance, 0.01 Da MS/MS mass tolerance and an enzyme digest of trypsin with a maximum of three missed cleavages. Carbamidomethylation of cysteines was included as a fixed modification, and oxidation of methionine and protein N-terminal acetylation as variable modifications. The false discovery rate for protein identification was set to 1%. All mass spectrometry data can be accessed here: ftp://massive.ucsd.edu/MSV000083021. Annotation of the putative *S. mansoni* proteasome subunits with the α and β subunit nomenclature was performed by comparing sequence alignments against the human 20S proteasome subunits using BLAST 2.6.0+ command line tools.

Evaluation of carmaphycin B and analogs.

Carmaphycin B and 11 of the 20 analogs described by LaMonte et al[28] were screened at 50 nM with Sm20S and c20S. Inhibition assays were performed as described above with Suc-LLVY-AMC. Incubations of the parasite with carmaphycin B and analogs **1**, **5**, **7**, **10** and **17**, and the subsequent WormAssay were performed as described above. After 24 h, worms were recovered and lysates prepared for residual proteasome activity analysis, as described above.

Proteasome activity and inhibition assays.

Proteasome activity assays were performed using 0.29 nM of Sm20S, c20S or i20S with 25 μM of Suc-LLE-AMC, Suc-LRR-AMC or Suc-LLVY-AMC in 20 mM Tris-HCl, pH 7.5 assay buffer. Assays with Suc-LLVY-AMC and Suc-LLE-AMC also contained 0.02% SDS. SDS was omitted from the Suc-LRR-AMC assays as it is incompatible with this substrate. For 50 nM single concentration inhibition assays of Sm20S, inhibitor and substrate were added the simultaneously to the enzyme and the rate of AMC release was determined from 60 to 120 minutes and compared to a DMSO control. For dose-response inhibition assays, an eight-point serial dilution of inhibitors in DMSO was acoustically transferred to 384w assay plates using an ATS Gen 4 Plus (Biosero, San Diego, CA). The enzyme and substrate, in assay buffer, were added simultaneously to the assay plate with a Biomek FX^P workstation equipped with a 96 multichannel pipetting head (Beckman Coulter, Brea, CA), and the rate of fluorophore release was monitored for 4 h compared to a DMSO control. IC_{50} values were calculated in GraphPad Prism 6 by normalizing activity to DMSO controls and interpolating the data using the log(inhibitor) – variable slope curve fitting algorithm.

Chapter 2, in full, is a reprint of the material as it appears in The Proteasome as a Drug Target in the Metazoan Pathogen, *Schistosoma mansoni*. Bibo-Verdugo, Betsaida; Wang, Steven;

Almaliti, Jehad; Ta, Anh; Jiang, Zhenze; Wong, Derek; Lietz, Christopher; Suzuki, Brian; El-Sakkary, Nelly; Hook, Vivian; Salvesen, Guy; Gerwick, William; Caffrey, Conor; O'Donoghue, Anthony; ACS Infectious Diseases, 2019. The thesis author was the joint first author of this paper.

RESULTS

Human proteasome inhibitors induce phenotypic changes, including decreased motility, in *Schistosoma mansoni*.

MG132 is a reversible, tripeptide-aldehyde proteasome inhibitor that induces apoptosis in mammalian cells[42]. Previous studies have shown that this inhibitor causes global gene expression changes when co-incubated in culture with *S. mansoni*[43]. Using a quantitative motility assay, known as WormAssay[44], incubation of the mixed-sex adults with 1 µM MG132 for up to 24 h did not alter motility compared to DMSO-exposed controls (Figure 1A). When viewed under the microscope at 72 h, male and female worms were paired, were attached to the well surface by their oral and/or ventral suckers, and appeared normal in shape, movement and color (Supplementary Video 1) compared to DMSO controls (Supplementary Video 2). In contrast, treatment with 1 µM of bortezomib, a covalent, reversible, dipeptide boronic acid inhibitor of human proteasome[45], significantly decreased parasite motility by 45% and 87% after 6 h and 24 h, respectively (Figure 1A). By 72 h, the parasites were relatively motionless, unable to extend or flex their bodies and darkened, and had detached from the surface of the well (Supplementary Video 3). Bortezomib can react with serine hydrolases[46], which leaves open the question of whether the phenotypic responses recorded were in fact due to proteasome inhibition alone. Therefore, we also tested the tetrapeptide epoxyketone inhibitor carfilzomib, an agent used to treat multiple myeloma[47] that exclusively reacts with the active site threonine residue found only in the proteasome[46]. At 1 µM, carfilzomib decreased worm motility by 47% and 89% after 6 h and 24 h, respectively. By 72 h, phenotypic changes were similar to those observed for bortezomib.

In mammalian cells, inhibition of the proteasome induces apoptosis including increased caspase activity[48,49]. Previously, our group measured an increase in caspase activity that was

associated with death of *S. mansoni* adult worms following *in vitro* exposure to statin drugs[50]. Therefore, we prepared lysates from worms that had been incubated for 24 h in the presence of 1 μM MG132, bortezomib or carfilzomib and measured activity of the executioner caspases of apoptosis with the fluorogenic substrate, Ac-DEVD-AFC. Caspase activity in worms exposed to MG132 was not significantly different from the DMSO control (Figure 1B). In contrast, bortezomib and carfilzomib induced a significant increase in caspase activity (7- and 4.5-fold, respectively) compared to the DMSO control. Thus, for the three proteasome inhibitors tested, the consistency noted between the appearance of phenotypic changes, decreased motility and increased caspase activity suggested that the schistosome proteasome was being engaged, a hypothesis that encouraged further biochemical characterization of the putative enzyme target.

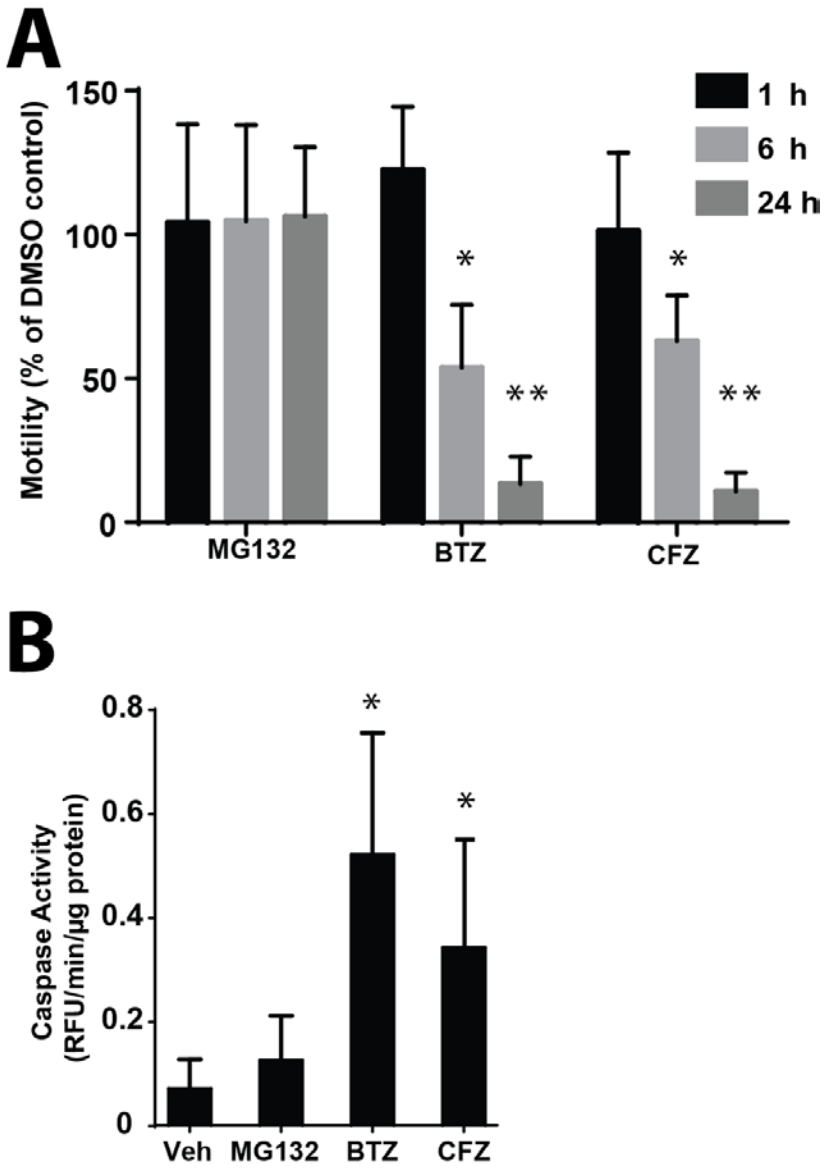

Figure 1: Proteasome inhibitors decrease worm motility and induce caspase activity. Experiments employed 24 well plates with 5-6 adult *S. mansoni* pairs per well. **A.** At each time point, WormAssay recordings were taken over 45 - 60 sec and the mean motility value per well noted. For bortezomib (BTZ) and carfilzomib (CFZ), the decrease in motility at 6 and 24 h relative to the 1 h time point is significant (*$p < 0.05$; ** $p < 0.005$) by the Student's *t*-test. **B.** Protein lysates were generated from *S. mansoni* worms following 24 h treatment with vehicle (Veh; 0.0001% DMSO) or 1 µM proteasome inhibitors. Caspase activity was quantified using the fluorescent peptide substrate, Ac-DEVD-AFC. Caspase activity (relative fluorescent units/min/µg) was significantly (*$p < 0.05$) increased in lysates from worms treated with bortezomib and carfilzomib (but not MG132) compared to vehicle control. Data shown are from experiments performed in triplicate: in one experiment, duplicate wells were used per treatment, whereas in the second and third experiments, quadruplicate wells were used, thus yielding a total of 10 wells per treatment.

Human proteasome inhibitors engage the proteasome in *S. mansoni*.

In the human proteasome, the subunits responsible for peptide hydrolysis are β1, β2 and β5, and each subunit has a distinct substrate preference[51]. The β1 subunit generally cleaves on the carboxyl terminal side of acidic residues whereas the β2 subunit preferentially cleaves after basic residues. Most proteasome inhibitors, including MG132, bortezomib and carfilzomib, target the β5 subunit. This subunit generally cleaves on the carboxyl terminal side of hydrophobic residues[52] and is typically monitored using the fluorogenic substrate, Succinyl-Leu-Leu-Val-Tyr-7-amido-4-methylcoumarin (Suc-LLVY-AMC). Under the same assay conditions, Suc-LLVY-AMC may also be cleaved by cysteine proteases such as calpains[53] that are present in *S. mansoni*[54]. To eliminate the cysteine protease activity, protein lysates from mixed-sex adult worms were prepared in a buffer containing 100 μM of E-64, a broad acting cysteine protease inhibitor. When the worm lysate was then assayed with Suc-LLVY-AMC, proteolytic activity was reduced by 92%, 99% and 100% in the presence 1 μM of MG132, bortezomib or carfilzomib, respectively (Figure 2A). As each of these inhibitors have different chemical reactive groups and all are predicated to target the β5 proteasome subunit, we can conclude that all of the proteolytic activity being measured with Suc-LLVY-AMC in parasite extracts is due to proteasome activity.

Having confirmed the assay conditions to specifically measure parasite β5 activity, we evaluated whether MG132, bortezomib and carfilzomib engage the proteasome in living *S. mansoni*. Parasites were exposed to 1 μM of each inhibitor for 24 h. After extensive washing, worm extracts were prepared and assayed for proteasome activity using Suc-LLVY-AMC. Activity was normalized to protein concentration. Bortezomib and carfilzomib decreased proteasome activity by 76% and 84%, respectively (Figure 2B). In contrast, MG132 had no effect on proteasome activity. These data demonstrate that bortezomib and carfilzomib but not MG132,

engage the intended target in living worms. Furthermore, their inhibition of the target is associated with the major phenotypic and biochemical changes described above.

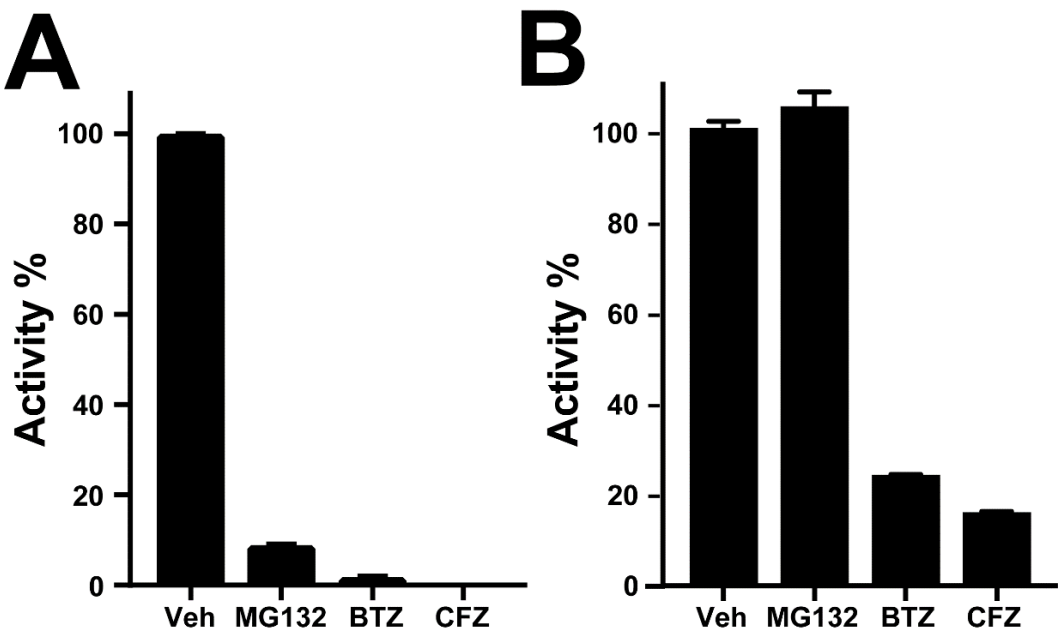

Figure 2: *S. mansoni* proteasome β5 subunit activity and its inhibition in living parasites. **A**. Proteolytic activity in *S. mansoni* adult lysate was measured with the Suc-LLVY-AMC substrate. Proteolytic activity was reduced by >95% in the presence of 1 μM MG132, bortezomib (BTZ) or carfilzomib (CFZ) compared to a vehicle (Veh) control assay consisting of 0.0001% DMSO. **B.** Adult *S. mansoni* worms (5-6 pairs per well) were incubated with 1 μM of MG132, BTZ or CFZ for 24 h. After extensive washing, protein extracts were prepared and assayed with Suc-LLVY-AMC. Proteasome activity was normalized to protein concentration across all groups and activity expressed as a percentage relative to vehicle (Veh) control (0.05% DMSO). Data are presented as the mean ± SD from triplicate experiments each performed in duplicate.

Enrichment of active proteasome from *S. mansoni* lysates.

To enrich for the *S. mansoni* proteasome (Sm20S), we developed a protocol using two chromatographic separation steps. Adult mixed-sex worm lysates were fractionated via gel filtration chromatography followed by DEAE-anion exchange column chromatography and activity was monitored using Suc-LLVY-AMC (Figure 3A). Attempts to enrich the proteasome further using cation exchange or hydrophobic interaction chromatography did not yield active

enzyme in the eluted fractions. Therefore, fractions from the DEAE-anion exchange column containing the most abundant activity were pooled and resolved by SDS-PAGE followed by silver staining (Figure 3B).

Two gel slices were excised for mass spectrometry analysis (Figure 3B). Gel Slice 1 contained numerous proteins in the range of 25-40 kDa that correspond in size to the α and β subunits of the human constitutive proteasome (c20S) and the human immunoproteasome (i20S). Fourteen putative 20S subunits were identified and each of these shared more than 46% sequence homology with a single *S. mansoni* proteasome subunit. The close alignment of proteasome subunits allowed us to assign a number to each *S. mansoni* subunit using the human proteasome nomenclature (Figure 3C). The active site triad consisting of Thr-1, Asp-17 and Lys-33 found in the c20S β1, β2 and β5 subunits[55] is conserved within the subunits of the Sm20S counterparts indicating that the parasite proteasome has 3 catalytically active β subunits (Figure 3D).

Gel slice 2 contained many high molecular weight proteins in the range of 60-110 kDa. Among a number of diverse proteins identified by mass spectrometry, six regulatory subunits of the *S. mansoni* proteasome were found (Supplementary File 1). Taken together, these data confirm that the core 20S proteasome and its associated regulatory subunits are enriched from adult worm lysates using a two-step column chromatography protocol.

Figure 3: Enrichment of Sm20S from *S. mansoni* protein extracts.
A. A two-step protocol involving gel filtration followed by DEAE-anion exchange chromatography was employed to enrich for Sm20S from *S. mansoni* lysates. Protein was separated on a Superose-6 10/300 gel filtration column and fractions with activity against Suc-LLVY-AMC were pooled (red shaded area). The pooled fractions were separated on a DEAE column and active fractions were again pooled (red shaded area). **B**. Pooled fractions containing Sm20S were resolved by SDS-PAGE beside the human immunoproteasome (i20S) and constitutive proteasome (c20S). Following silver staining, two gel slices, indicated in brackets, were excised for proteomic analysis. **C**. Dendogram showing the protein sequence homology between the human c20S proteasome subunits and those identified for Sm20S in gel slice 1. The UniProt identifiers for the Sm20S and c20S subunits are indicated in blue and black, respectively. **D.** Protein sequence alignment of residues 1 to 35 of β1, β2 and β5 subunits from Sm20S (blue) and c20S (black). The amino acids involved in catalytic activity of c20S are underlined and conserved in Sm20S.

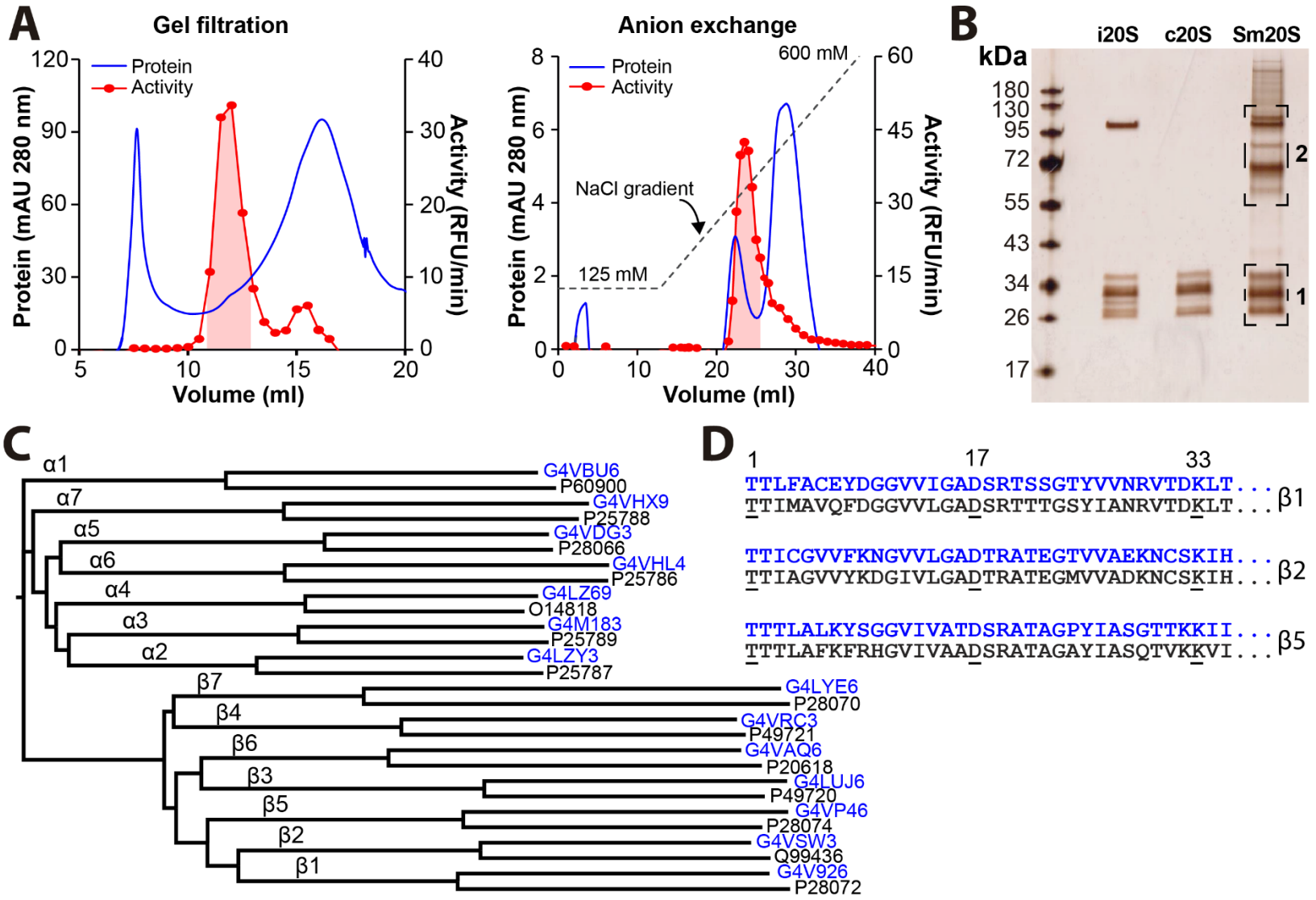
A
Gel filtration
Protein
Activity
Protein (mAU 280 nm)
Activity (RFU/min)
Volume (ml)
Anion exchange
600 mM
NaCl gradient
125 mM
B
kDa
i20S
c20S
Sm20S
180
130
95
72
55
43
34
26
17
2
1
C
α1
α7
α5
α6
α4
α3
α2
β7
β4
β6
β3
β5
β2
β1
G4VBU6
P60900
G4VHX9
P25788
G4VDG3
P28066
G4VHL4
P25786
G4LZ69
O14818
G4M183
P25789
G4LZY3
P25787
G4LYE6
P28070
G4VRC3
P49721
G4VAQ6
P20618
G4LUJ6
P49720
G4VP46
P28074
G4VSW3
Q99436
G4V926
P28072
D
1
17
33
TTLFACEYDGGVVIGADSRTSSGTYVVNRVTDKLT...
TTIMAVQFDGGVVLGADSRTTTGSYIANRVTDKLT...
β1
TTICGVVFKNGVVLGADTRATEGTVVAEKNCSKIH...
TTIAGVVYKDGIVLGADTRATEGMVVADKNCSKIH...
β2
TTTLALKYSGGVIVATDSRATAGPYIASGTTKKII...
TTTLAFKFRHGVIVAADSRATAGAYIASQTVKKVI...
β5

Subunit characterization of the *S. mansoni* proteasome.

Sm20S was enriched from *S. mansoni* lysates by monitoring for β5 chymotrypsin-type activity using the substrate, Suc-LLVY-AMC. The concentration of this enzyme complex was determined by active site titration with carfilzomib. Using 5 nM of Sm20S, we then compared the β5 activity to an equal molar concentration of c20S and i20S. The human enzymes cleaved Suc-LLVY-AMC at 35- to 40-fold faster rate than Sm20S.Proteomic data indicated that the caspase-type (β1: G4V926) and trypsin-type (β2: G4VSW3) catalytic subunits were also present and likely enzymatically active due to the presence of a conserved electrophilic threonine residue. Therefore, we predicted that the enriched Sm20S could cleave the human β1 caspase-type substrate, z-LLE-AMC, and the human β2 trypsin-type substrate, z-LRR-AMC[56]. Using an equal concentration of Sm20S, c20S and i20S, we compared their activities with the β1 and β2 fluorogenic substrates and found that the human proteasomes cleaved both substrates more rapidly than the parasite proteasome (Figure 4A).

We next measured the potency of bortezomib and carfilzomib against Sm20S. Bortezomib inhibited the β1, β2 and β5 subunits of Sm20S with IC_{50} values of 15 nM, 272 nM and 9 nM, respectively (Figure 4B). In contrast, carfilzomib was more than 33-fold less potent against the β1 subunit (IC_{50} = >500 nM) when compared to bortezomib, however, it was 5.6-fold more potent against the β2 subunit (IC_{50} = 48 nM) and 18-fold more potent against the β5 subunit (IC_{50} = 0.5 nM) (Figure 4C). Although these compounds are potent inhibitors of Sm20S activity and have different selectivity for each of the subunits, they are generally cytotoxic to mammalian cells. This cytotoxicity limits their potential use as anthelmintics. Therefore, we evaluated additional inhibitors that have been developed for non-human proteasome targets.

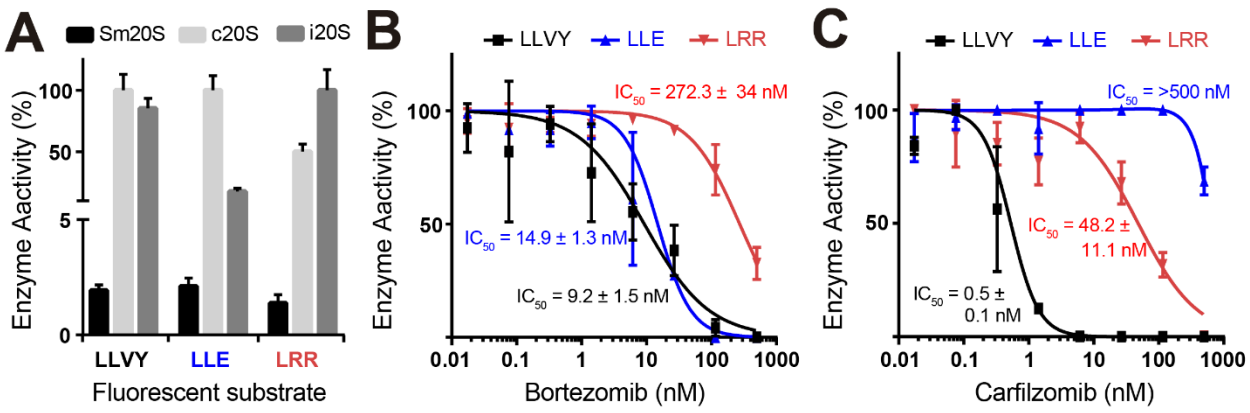

Figure 4: Substrate and inhibitor profiling the catalytic subunits of Sm20S.
A. Activity assays with subunit-selective proteasome substrates for β1 (LLE), β2 (LRR) and β5 (LLVY). **B.** Determination of bortezomib potency with Sm20S using subunit-selective substrates. **C.** Determination of carfilzomib potency with Sm20S using the same substrates. Data for **A**, **B** and **C** are from one assay performed in triplicate: means ± SEM values are shown.

The carmaphycin B scaffold as a basis to develop novel Sm20S inhibitors.

Carmaphycin B is a marine natural product isolated from cyanobacterium consisting of P3-Val, P2-Met sulfone and P1-Leu capped with an epoxyketone group on the carboxyl terminus and an N-hexanoyl cap group on the amino terminus[30] (Figure 5A). Carmaphycin B inhibits Sm20S β2 and β5 activity with IC_{50} values of = 0.6 and 10 nM respectively and only partially inhibits β1 activity at 500 nM (Figure 5A)). This compound also potently inhibits human the β5 subunits of c20S and i20S β2 with IC_{50} values of less than 5 nM but is 5-fold more potent for targeting the β2 subunit of c20S compared to β2 of i20S (IC_{50} = 12 nM v 62 nM). Carmaphycin B is toxic to HepG2 cells with a 24 h EC_{50} value of 12.6 nM (Figure 5B) however, we previously developed a set of 20 carmaphycin B analogs to target the *Plasmodium falciparum* proteasome of which 11 demonstrated decreased HepG2 cytotoxicity, ranging from 31 nM to 3410 nM[28]. Sm20Swas assayed with 50 nM of these 11 compounds and the percentage inhibition determined using the β5 substrate, Suc-LLVY-AMC. As expected, carmaphycin B completely inhibited Sm20S at this concentration, and only compounds 1, 7, and 17 decreased activity by more than 40%.

Concentration-response curves were generated for compounds 1, 7 and 17 with Sm20S, c20S and i20S (Figure 5C) to determine if any of these compounds were more potent against the parasite proteasome relative to the human proteasomes. Unlike bortezomib, these compounds did not inhibit the β1 subunit at 500 nM (Supplementary Figure X). Analog 1 differs from carmaphycin B, by the substitution of P2 norleucine (Nle) for Met sulfone that results in an 11-fold reduction in HepG2 cytotoxicity. Using the β2 and β5 substrates, there was no difference in potency of analog 1 between the c20S and *S. mansoni* proteasome (Figure 5C) and it was less potent against the i20S subunits. Analog 7 also contains Nle in the P2 position, but has a substitution of Phe for Leu in P1 and Phe for Val in P3. Again, this compound had similar potency against the β5 subunits of c20S and Sm20S and lower potency against i20S β5. Analog 7 did not inhibit i20S β2 but was 3.3-fold more potent against Sm20S β2 compared to c20S β2 (Figure 5D). Finally, analog 17, which consists of Trp-Trp-Phe at the P3-P2-P1 positions had equal potency for the β5 subunits of all three proteasomes, however it selectively inhibited the β2 subunit of Sm20S (Figure 5E). As analogs 7 and 17 showed the greatest selectivity for the parasite proteasome and therefore were further characterized with adult worms.

Figure 5: A screen of carmaphycin B and 11 analogs identifies a compound that preferentially inhibits Sm20S with decreased cytotoxicity to human cells.
A. Inhibition of β5 chymotrypsin-type activity and β1 caspase-type activity of Sm20S by carmaphycin B. **B.** Heat map generated from inhibition assay data for Sm20S and c20S using carmaphycin B and 11 analogs (numbering system taken from LaMonte et al[28]). Enzyme was simultaneously mixed with Suc-LLVY-AMC and 50 nM inhibitor. Remaining activity was measured after 1 h and normalized to that of the control containing 0.5% DMSO. The HepG2 EC_{50} data were reported previously[28]. **C-E**. Concentration response curves for carmaphycin B analogs **1**, **7** and **17** using Suc-LLVY-AMC.

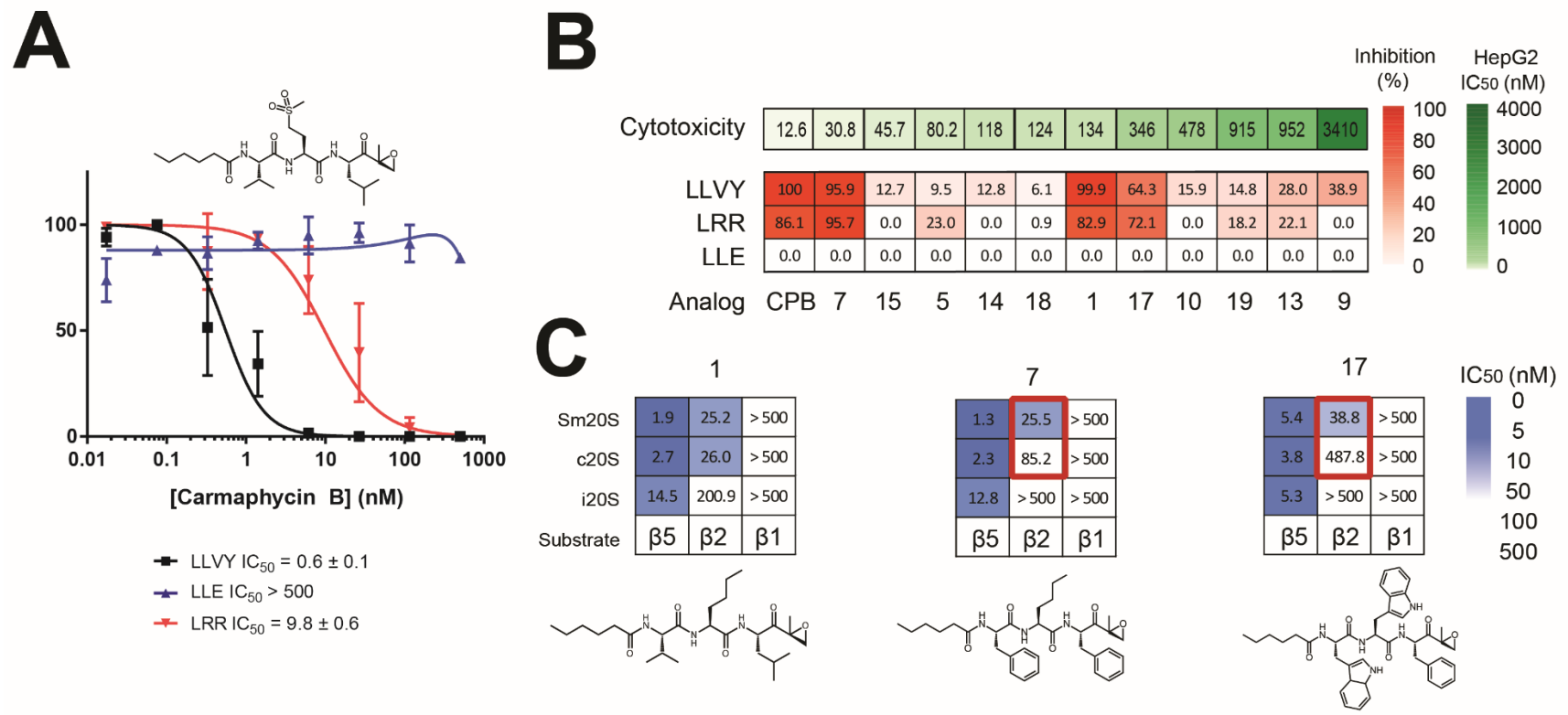
A
100
50
0
0.01
0.1
1
10
100
1000
[Carmaphycin B] (nM)
LLVY IC50 = 0.6 ± 0.1
LLE IC50 > 500
LRR IC50 = 9.8 ± 0.6
B
Inhibition (%)
HepG2 IC50 (nM)
Cytotoxicity 12.6 30.8 45.7 80.2 118 124 134 346 478 915 952 3410
LLVY 100 95.9 12.7 9.5 12.8 6.1 99.9 64.3 15.9 14.8 28.0 38.9
LRR 86.1 95.7 0.0 23.0 0.0 0.9 82.9 72.1 0.0 18.2 22.1 0.0
LLE 0.0 0.0 0.0 0.0 0.0 0.0 0.0 0.0 0.0 0.0 0.0 0.0
Analog CPB 7 15 5 14 18 1 17 10 19 13 9
C
1
Sm20S 1.9 25.2 > 500
c20S 2.7 26.0 > 500
i20S 14.5 200.9 > 500
Substrate β5 β2 β1
7
1.3 25.5 > 500
2.3 85.2 > 500
12.8 > 500 > 500
β5 β2 β1
17
5.4 38.8 > 500
3.8 487.8 > 500
5.3 > 500 > 500
β5 β2 β1
IC50 (nM)
0
5
10
50
100
500

Activity of carmaphycin analogs against *S. mansoni in vitro.*

The anti-schistosomal activity of carmaphycin B and analogs 7 and 17, were evaluated at 1 μM using mixed-sex adult *S. mansoni* in culture. These compounds were compared to analogs 5 and 10 that were found to be weaker inhibitors of Sm20S and did not target the β1 or β2 subunit at 500 nM (Supplementary Figure 1). Bortezomib was included as a positive control. After 24 h, bortezomib, carmaphycin B, 7 and 17 decreased worm movement by at least 80% (Figure 6A) and generated the same deleterious phenotypic changes previously noted for bortezomib. These changes were associated with inhibition of the Sm20S β5 activity by 80% or more (Figure 6B). In contrast, analogs 5 and 10 decreased motility by just 22% and 40%, respectively, and no obvious phenotypic changes were observed. Also, β5 subunit activity was reduced by 52% and 70%, respectively. Overall, there was strong correlation between proteasome inhibition and worm motility (Pearson correlation coefficient = 0.922), indicating that engagement of the schistosome proteasome target is responsible for the particular phenotypic response. When comparing compounds 7 and 17, the latter has stronger phenotypic performance, increased selectivity for Sm20S over c20S and i20S and lower HepG2 cytotoxicity. Therefore 17 was identified as an ideal starting point for the future design of more potent and selective inhibitors of Sm20S.

Chapter 3, in full, is a reprint of the material as it appears in The Proteasome as a Drug Target in the Metazoan Pathogen, *Schistosoma mansoni*. Bibo-Verdugo, Betsaida; Wang, Steven; Almaliti, Jehad; Ta, Anh; Jiang, Zhenze; Wong, Derek; Lietz, Christopher; Suzuki, Brian; El-Sakkary, Nelly; Hook, Vivian; Salvesen, Guy; Gerwick, William; Caffrey, Conor; O'Donoghue, Anthony; ACS Infectious Diseases, 2019. The thesis author was the joint first author of this paper.

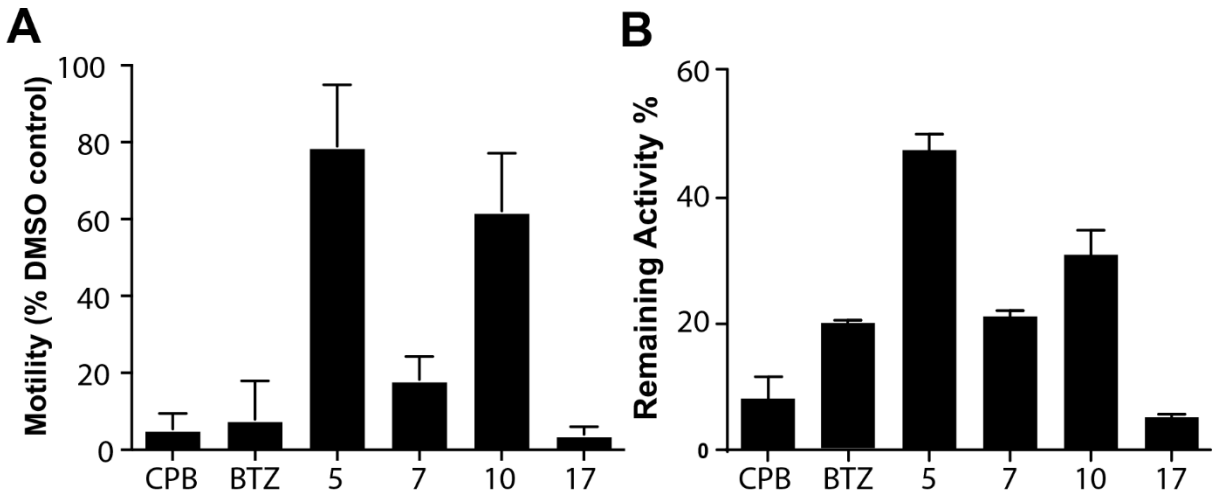

Figure 6: Decreased parasite motility in the presence of carmaphycin B and its analogs correlates with inhibition of the proteasome. A. Experiments employed 24 well plates with 5-6 adult *S. mansoni* pairs per well and 1 µM of carmaphycin B (CPB), bortezomib (BTZ) and the indicated analogs. After 24 h, WormAssay recordings were taken over 45-60 sec and the mean motility value per well noted. **B.** The same worms used in **A** were extensively washed and protein extracts prepared in the presence of 100 µM E-64 for assay with Suc-LLVY-AMC. Proteasome activity was normalized to protein concentration across all groups and activity expressed as the percentage activity of the remaining activity relative to DMSO controls. Data are presented as means ± SEM from three experiments each in triplicate.

DISCUSSION

In spite of the strong conservation of the ubiquitin-proteasome system among eukaryotes, recent reports demonstrate that potent proteasome inhibitors can be designed with selectivity for pathogens over the human host. In particular, much effort has be made to target the *Plasmodium* proteasome with epoxyketone[28,57], vinyl sulfone[58,59] and ethylenediamine[60] inhibitors. From these studies, compounds with more than 380-fold selectivity for *Plasmodium falciparum* over mammalian cells have emerged[28,60]. Further, a large-scale library screening and medicinal chemistry effort led to the development of non-competitive proteasome inhibitors that selectively target the kinetoplastid parasites responsible for leishmaniasis, Chagas disease, and sleeping sickness[29]. Using these studies as a precedent, we anticipated that the proteasome in *S. mansoni* could also be a target for the development of potent and selective proteasome inhibitors.

Previous genetic[61] and chemical evidence[43,62] suggest that the *S. mansoni* proteasome is important for the establishment of infection in the mammalian host. Also, gene expression studies have communicated the biological importance of the schistosome ubiquitin proteasome system during oxidative stress and heat shock conditions[63] and for egg development and morphology[64]. Here, we focused on adult parasites as they are ultimately responsible for disease morbidity via the eggs they produce. We showed that 1 μM of either bortezomib or carfilzomib inhibited proteasome activity in a worm lysate and caused pronounced phenotypic and biochemical changes to adult *S. mansoni*. MG132 also inhibited proteasome activity in the lysate but did not cause any phenotypic or biochemical changes to the worm. The lack of potency in the worm motility assays may be due to poor penetration of this compound in the worm or the aldehyde group is oxidized rapidly within the worm, as has been shown in mouse studies[65]. In addition, MG132 reacts with papain-fold cysteine proteases[66,67] and these enzymes are abundantly expressed in *S. mansoni* adult

worms[68]. Therefore, cysteine proteases may sequester much of the MG132 thereby reducing the inhibitor concentration that can interact with the proteasome.

The result contrasts with the significant reduction in the survival of *S. mansoni* larvae post-exposure to MG132[62], where a 50-times higher concentration was used. The decrease in parasite survival after exposure to a high concentration of MG132 may be due to the dual inhibition of the proteasome and papain-type cysteine proteases as was seen in studies with *P. falciparum*[67]. Here, we observed for bortezomib and carfilzomib, a clear association between the phenotypic changes in adult *S. mansoni*, the induction of caspase activity and engagement of the proteasome target. This encouraged us to isolate and biochemically characterize Sm20S.

Sm20S was enriched from adult worm lysates and all subunits were identified by proteomic analysis and annotated based on sequencing similarity with the human proteasome. The protein sequence analysis revealed that the Sm20S complex has all of the amino acids associated with the catalytic triad of human β1, β2 and β5 subunits[55]. The schistosome enzyme complex readily hydrolyzed the standard β1 caspase-type, β2 trypsin-type and β5 chymotrypsin-type substrates albeit a different rate to the human constitutive and immune proteasomes. These substrate specificity and turnover data indicate that there may be subtle differences between the *S. mansoni* and human proteasome that could be exploited for inhibitor development.

Using the available substrates, we found that bortezomib inhibits Sm20S β1 and β5 subunits with equal potency, whereas the epoxyketone inhibitor, carfilzomib, has approximately 100-fold and 1000-fold selectivity for the β5 subunit over the β2 and β1 subunits, respectively**.** These data reveal that the similar phenotypic and biochemical changes in adult *S. mansoni* that were recorded in the presence of these inhibitors, involve targeting of the β5 subunit and second subunit, either β1 or β2. Peptide vinyl sulfone inhibitors that were developed to target the

Plasmodium proteasome inhibited both the β5 and β2 subunits[58,59] but inhibition of β2 alone was insufficient to kill the parasite[60]. The exact contribution of the Sm20S β1 and β2 subunits to schistosome survival is unknown as we have yet to identify compounds that specifically target these individual subunits.

In order to discover proteasome inhibitors that engage Sm20S but have reduced toxicity to host mammalian cells, we screened a library of peptide-epoxyketone compounds derived from the marine natural product, carmaphycin B[30]. This library previously yielded a tri-peptide epoxyketone inhibitor with a 379-fold selectivity for *P. falciparum* over HepG2 cells[28]. The lead anti-malarial compound, 18, consisted of D-valine, L-norleucine and L-leucine in the P3, P2 and P1 positions, respectively. This compound weakly inhibited Sm20S β5 with an IC_{50} value of 474 nM, thereby indicating that there are clear differences between the β5 subunits of these parasite-derived proteasomes. Our enzyme activity screen identified hit compounds (1, 7 and 17) all of which contain L-amino acids in the P3 position. In the activity assays, compound 17 targeted Sm20S β5 and β2 subunits and was selective molecule for relative to c20S. In addition, it was more potently anti-schistosomal and displayed reduced cytotoxicity compared to 1 and 7. Our future studies will aim to improve the attributes of 17 regarding potency, selectivity and safety. With this in mind, the recent development of orally bioavailable peptide boronic acid[69] proteasome inhibitors to treat multiple myeloma is encouraging and consistent with the target product profile for new anti-schistosomals (and other anthelmintics) that demands orally active drugs[70,71].

Chapter 4, in full, is a reprint of the material as it appears in The Proteasome as a Drug Target in the Metazoan Pathogen, *Schistosoma mansoni*. Bibo-Verdugo, Betsaida; Wang, Steven; Almaliti, Jehad; Ta, Anh; Jiang, Zhenze; Wong, Derek; Lietz, Christopher; Suzuki, Brian; El-

Sakkary, Nelly; Hook, Vivian; Salvesen, Guy; Gerwick, William; Caffrey, Conor; O'Donoghue, Anthony; ACS Infectious Diseases, 2019. The thesis author was the joint first author of this paper.

CONCLUSION

This research demonstrates that treatment of adult *S. mansoni* worms with FDA-approved proteasome inhibitors cause significant phenotypic and biochemical changes to the worms. These anti-cancer drugs are broadly cytotoxic to mammalian cells, therefore we screened a selection of natural product-derived proteasome inhibitors that have reduced mammalian cytotoxicity. From this screen, we identified a hit molecule that has 10-fold selectivity for the *S. mansoni* proteasome over the human proteasome. We show that treatment of adult *S. mansoni* with this inhibitor causes the same phenotypic response as the FDA-approved drugs and that these phenotypic changes are directly due to engagement of the target enzyme.

Chapter 5, in full, is a reprint of the material as it appears in The Proteasome as a Drug Target in the Metazoan Pathogen, *Schistosoma mansoni*. Bibo-Verdugo, Betsaida; Wang, Steven; Almaliti, Jehad; Ta, Anh; Jiang, Zhenze; Wong, Derek; Lietz, Christopher; Suzuki, Brian; El-Sakkary, Nelly; Hook, Vivian; Salvesen, Guy; Gerwick, William; Caffrey, Conor; O'Donoghue, Anthony; ACS Infectious Diseases, 2019. The thesis author was the joint first author of this paper.

APPENDIX

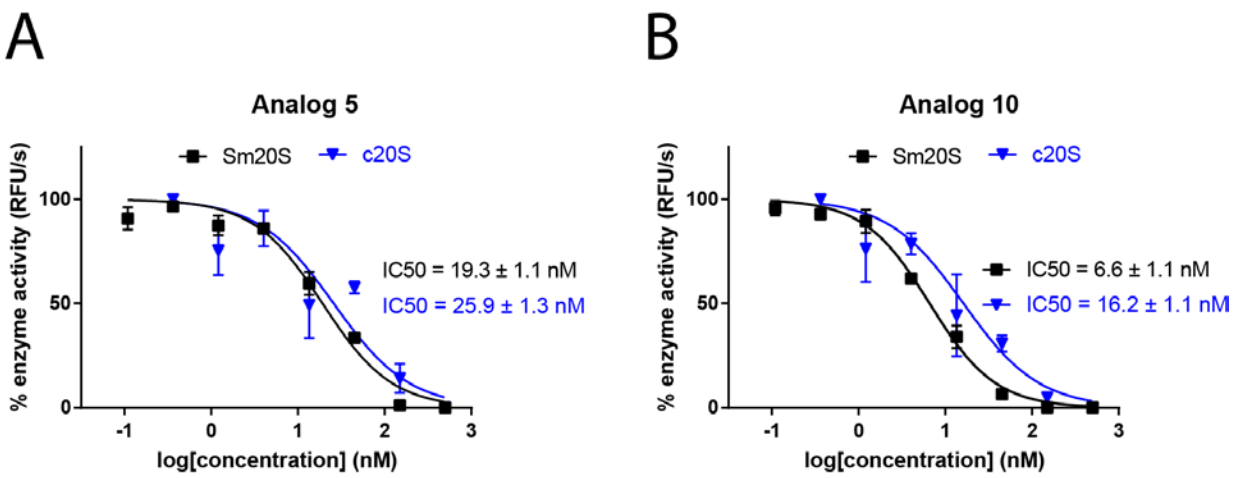

Supplementary Figure 1: Concentration response curves for carmaphycin B analogs 5 and 10 using Suc-LLVY-AMC

A. Inhibition of β5 chymotrypsin-type activity of Sm20S and c20S by analog 5. **B.** Inhibition of β5 chymotrypsin-type activity of Sm20S and c20S by analog 10.

REFERENCES

(1) Gryseels, B.; Polman, K.; Clerinx, J.; Kestens, L. Human Schistosomiasis. *Lancet (London, England)* **2006**, *368* (9541), 1106–1118. https://doi.org/10.1016/S0140-6736(06)69440-3.

(2) Colley, D. G.; Bustinduy, A. L.; Secor, W. E.; King, C. H. Human Schistosomiasis. *Lancet (London, England)* **2014**, *383* (9936), 2253–2264. https://doi.org/10.1016/S0140-6736(13)61949-2.

(3) McManus, D. P.; Dunne, D. W.; Sacko, M.; Utzinger, J.; Vennervald, B. J.; Zhou, X.-N. Schistosomiasis. *Nat. Rev. Dis. Prim.* **2018**, *4* (1), 13. https://doi.org/10.1038/s41572-018-0013-8.

(4) Lewis, F. A.; Tucker, M. S. Schistosomiasis. *Adv. Exp. Med. Biol.* **2014**, *766*, 47–75. https://doi.org/10.1007/978-1-4939-0915-5_3.

(5) Ross, A. G. P.; Bartley, P. B.; Sleigh, A. C.; Olds, G. R.; Li, Y.; Williams, G. M.; McManus, D. P. Schistosomiasis. *N. Engl. J. Med.* **2002**, *346* (16), 1212–1220. https://doi.org/10.1056/NEJMra012396.

(6) Lu, Z.; Sessler, F.; Holroyd, N.; Hahnel, S.; Quack, T.; Berriman, M.; Grevelding, C. G. Schistosome Sex Matters: A Deep View into Gonad-Specific and Pairing-Dependent Transcriptomes Reveals a Complex Gender Interplay. *Sci. Rep.* **2016**, *6*, 31150. https://doi.org/10.1038/srep31150.

(7) Haeberlein, S.; Haas, W. Chemical Attractants of Human Skin for Swimming Schistosoma Mansoni Cercariae. *Parasitol. Res.* **2008**, *102* (4), 657–662. https://doi.org/10.1007/s00436-007-0807-1.

(8) McKerrow, J. H.; Jones, P.; Sage, H.; Pino-Heiss, S. Proteinases from Invasive Larvae of the Trematode Parasite Schistosoma Mansoni Degrade Connective-Tissue and Basement-Membrane Macromolecules. *Biochem. J.* **1985**, *231* (1), 47–51.

(9) Wilson, R. A.; Coulson, P. S. Schistosoma Mansoni: Dynamics of Migration through the Vascular System of the Mouse. *Parasitology* **1986**, *92 (Pt 1)*, 83–100.

(10) Fulford, A. J.; Butterworth, A. E.; Ouma, J. H.; Sturrock, R. F. A Statistical Approach to Schistosome Population Dynamics and Estimation of the Life-Span of Schistosoma Mansoni in Man. *Parasitology* **1995**, *110 (Pt 3*, 307–316.

(11) Payet, B.; Chaumentin, G.; Boyer, M.; Amaranto, P.; Lemonon-Meric, C.; Lucht, F. Prolonged Latent Schistosomiasis Diagnosed 38 Years after Infestation in a HIV Patient. *Scand. J. Infect. Dis.* **2006**, *38* (6–7), 572–575. https://doi.org/10.1080/00365540500444660.

(12) Potters, I.; Van Duffel, L.; Broeckx, G.; Bottieau, E. Intestinal Schistosomiasis: A Very

Long-Lived Tropical Parasite. *Clin. Microbiol. Infect.* **2019**. https://doi.org/10.1016/j.cmi.2019.02.014.

(13) Molyneux, D. H.; Savioli, L.; Engels, D. Neglected Tropical Diseases: Progress towards Addressing the Chronic Pandemic. *Lancet (London, England)* **2017**, *389* (10066), 312–325. https://doi.org/10.1016/S0140-6736(16)30171-4.

(14) Gray, D. J.; Ross, A. G.; Li, Y.-S.; McManus, D. P. Diagnosis and Management of Schistosomiasis. *BMJ* **2011**, *342*, d2651. https://doi.org/10.1136/bmj.d2651.

(15) Nour, N. M. Schistosomiasis: Health Effects on Women. *Rev. Obstet. Gynecol.* **2010**, *3* (1), 28–32.

(16) Ross, A. G.; Vickers, D.; Olds, G. R.; Shah, S. M.; McManus, D. P. Katayama Syndrome. *Lancet. Infect. Dis.* **2007**, *7* (3), 218–224. https://doi.org/10.1016/S1473-3099(07)70053-1.

(17) Doenhoff, M. J.; Cioli, D.; Utzinger, J. Praziquantel: Mechanisms of Action, Resistance and New Derivatives for Schistosomiasis. *Curr. Opin. Infect. Dis.* **2008**, *21* (6), 659–667. https://doi.org/10.1097/QCO.0b013e328318978f.

(18) Cioli, D.; Pica-Mattoccia, L. Praziquantel. *Parasitol. Res.* **2003**, *90 Supp 1*, S3-9. https://doi.org/10.1007/s00436-002-0751-z.

(19) Bibo-Verdugo, B.; Jiang, Z.; Caffrey, C. R.; O'Donoghue, A. J. Targeting Proteasomes in Infectious Organisms to Combat Disease. *FEBS J.* **2017**, *284* (10), 1503–1517. https://doi.org/10.1111/febs.14029.

(20) Nandi, D.; Tahiliani, P.; Kumar, A.; Chandu, D. The Ubiquitin-Proteasome System. *J. Biosci.* **2006**, *31* (1), 137–155.

(21) Tanaka, K. The Proteasome: Overview of Structure and Functions. *Proc. Jpn. Acad. Ser. B. Phys. Biol. Sci.* **2009**, *85* (1), 12–36.

(22) Winter, M. B.; La Greca, F.; Arastu-Kapur, S.; Caiazza, F.; Cimermancic, P.; Buchholz, T. J.; Anderl, J. L.; Ravalin, M.; Bohn, M. F.; Sali, A.; O'Donoghue, A. J.; Craik, C. S. Immunoproteasome Functions Explained by Divergence in Cleavage Specificity and Regulation. *Elife* **2017**, *6*. https://doi.org/10.7554/eLife.27364.

(23) Fehling, H. J.; Swat, W.; Laplace, C.; Kuhn, R.; Rajewsky, K.; Muller, U.; von Boehmer, H. MHC Class I Expression in Mice Lacking the Proteasome Subunit LMP-7. *Science* **1994**, *265* (5176), 1234–1237.

(24) Barton, L. F.; Runnels, H. A.; Schell, T. D.; Cho, Y.; Gibbons, R.; Tevethia, S. S.; Deepe, G. S. J.; Monaco, J. J. Immune Defects in 28-KDa Proteasome Activator Gamma-Deficient Mice. *J. Immunol.* **2004**, *172* (6), 3948–3954.

(25) Tanaka, K.; Kasahara, M. The MHC Class I Ligand-Generating System: Roles of

Immunoproteasomes and the Interferon-Gamma-Inducible Proteasome Activator PA28. *Immunol. Rev.* **1998**, *163*, 161–176.

(26) Steverding, D.; Wang, X. Trypanocidal Activity of the Proteasome Inhibitor and Anti-Cancer Drug Bortezomib. *Parasit. Vectors* **2009**, *2* (1), 29. https://doi.org/10.1186/1756-3305-2-29.

(27) Li, H.; van der Linden, W. A.; Verdoes, M.; Florea, B. I.; McAllister, F. E.; Govindaswamy, K.; Elias, J. E.; Bhanot, P.; Overkleeft, H. S.; Bogyo, M. Assessing Subunit Dependency of the Plasmodium Proteasome Using Small Molecule Inhibitors and Active Site Probes. *ACS Chem. Biol.* **2014**, *9* (8), 1869–1876. https://doi.org/10.1021/cb5001263.

(28) LaMonte, G. M.; Almaliti, J.; Bibo-Verdugo, B.; Keller, L.; Zou, B. Y.; Yang, J.; Antonova-Koch, Y.; Orjuela-Sanchez, P.; Boyle, C. A.; Vigil, E.; Wang, L.; Goldgof, G. M.; Gerwick, L.; O'Donoghue, A. J.; Winzeler, E. A.; Gerwick, W. H.; Ottilie, S. Development of a Potent Inhibitor of the Plasmodium Proteasome with Reduced Mammalian Toxicity. *J. Med. Chem.* **2017**, *60* (15), 6721–6732. https://doi.org/10.1021/acs.jmedchem.7b00671.

(29) Khare, S.; Nagle, A. S.; Biggart, A.; Lai, Y. H.; Liang, F.; Davis, L. C.; Barnes, S. W.; Mathison, C. J. N.; Myburgh, E.; Gao, M.-Y.; Gillespie, J. R.; Liu, X.; Tan, J. L.; Stinson, M.; Rivera, I. C.; Ballard, J.; Yeh, V.; Groessl, T.; Federe, G.; Koh, H. X. Y.; Venable, J. D.; Bursulaya, B.; Shapiro, M.; Mishra, P. K.; Spraggon, G.; Brock, A.; Mottram, J. C.; Buckner, F. S.; Rao, S. P. S.; Wen, B. G.; Walker, J. R.; Tuntland, T.; Molteni, V.; Glynne, R. J.; Supek, F. Proteasome Inhibition for Treatment of Leishmaniasis, Chagas Disease and Sleeping Sickness. *Nature* **2016**, *537* (7619), 229–233. https://doi.org/10.1038/nature19339.

(30) Pereira, A. R.; Kale, A. J.; Fenley, A. T.; Byrum, T.; Debonsi, H. M.; Gilson, M. K.; Valeriote, F. A.; Moore, B. S.; Gerwick, W. H. The Carmaphycins: New Proteasome Inhibitors Exhibiting an α,β-Epoxyketone Warhead from a Marine Cyanobacterium. *ChemBioChem* **2012**, *13* (6), 810–817. https://doi.org/10.1002/cbic.201200007.

(31) Duvall, R. H.; DeWitt, W. B. An Improved Perfusion Technique for Recovering Adult Schistosomes from Laboratory Animals. *Am. J. Trop. Med. Hyg.* **1967**, *16* (4), 483–486.

(32) Colley, D. G.; Wikel, S. K. Schistosoma Mansoni: Simplified Method for the Production of Schistosomules. *Exp. Parasitol.* **1974**, *35* (1), 44–51.

(33) Abdulla, M.-H.; Lim, K.-C.; Sajid, M.; McKerrow, J. H.; Caffrey, C. R. Schistosomiasis Mansoni: Novel Chemotherapy Using a Cysteine Protease Inhibitor. *PLoS Med.* **2007**, *4* (1), e14. https://doi.org/10.1371/journal.pmed.0040014.

(34) Abdulla, M.-H.; Ruelas, D. S.; Wolff, B.; Snedecor, J.; Lim, K.-C.; Xu, F.; Renslo, A. R.; Williams, J.; McKerrow, J. H.; Caffrey, C. R. Drug Discovery for Schistosomiasis: Hit and Lead Compounds Identified in a Library of Known Drugs by Medium-Throughput Phenotypic Screening. *PLoS Negl. Trop. Dis.* **2009**, *3* (7), e478.

https://doi.org/10.1371/journal.pntd.0000478.

(35) Basch, P. F.; Humbert, R. Cultivation of Schistosoma Mansoni in Vitro. III. Implantation of Cultured Worms into Mouse Mesenteric Veins. *J. Parasitol.* **1981**, *67* (2), 191–195.

(36) Marcellino, C.; Gut, J.; Lim, K. C.; Singh, R.; McKerrow, J.; Sakanari, J. WormAssay: A Novel Computer Application for Whole-Plate Motion-Based Screening of Macroscopic Parasites. *PLoS Negl. Trop. Dis.* **2012**, *6* (1), e1494. https://doi.org/10.1371/journal.pntd.0001494.

(37) Long, T.; Rojo-Arreola, L.; Shi, D.; El-Sakkary, N.; Jarnagin, K.; Rock, F.; Meewan, M.; Rascón, A. A.; Lin, L.; Cunningham, K. A.; Lemieux, G. A.; Podust, L.; Abagyan, R.; Ashrafi, K.; McKerrow, J. H.; Caffrey, C. R. Phenotypic, Chemical and Functional Characterization of Cyclic Nucleotide Phosphodiesterase 4 (PDE4) as a Potential Anthelmintic Drug Target. *PLoS Negl. Trop. Dis.* **2017**, *11* (7), 1–27. https://doi.org/10.1371/journal.pntd.0005680.

(38) Weeks, J. C.; Roberts, W. M.; Leasure, C.; Suzuki, B. M.; Robinson, K. J.; Currey, H.; Wangchuk, P.; Eichenberger, R. M.; Saxton, A. D.; Bird, T. D.; Kraemer, B. C.; Loukas, A.; Hawdon, J. M.; Caffrey, C. R.; Liachko, N. F. Sertraline, Paroxetine, and Chlorpromazine Are Rapidly Acting Anthelmintic Drugs Capable of Clinical Repurposing. *Sci. Rep.* **2018**, *8* (1), 975. https://doi.org/10.1038/s41598-017-18457-w.

(39) Glaser, J.; Schurigt, U.; Suzuki, B. M.; Caffrey, C. R.; Holzgrabe, U. Anti-Schistosomal Activity of Cinnamic Acid Esters: Eugenyl and Thymyl Cinnamate Induce Cytoplasmic Vacuoles and Death in Schistosomula of Schistosoma Mansoni. *Molecules* **2015**, *20* (6), 10873–10883. https://doi.org/10.3390/molecules200610873.

(40) Long, T.; Neitz, R. J.; Beasley, R.; Kalyanaraman, C.; Suzuki, B. M.; Jacobson, M. P.; Dissous, C.; McKerrow, J. H.; Drewry, D. H.; Zuercher, W. J.; Singh, R.; Caffrey, C. R. Structure-Bioactivity Relationship for Benzimidazole Thiophene Inhibitors of Polo-Like Kinase 1 (PLK1), a Potential Drug Target in Schistosoma Mansoni. *PLoS Negl. Trop. Dis.* **2016**, *10* (1), e0004356. https://doi.org/10.1371/journal.pntd.0004356.

(41) Shevchenko, A.; Tomas, H.; Havlis, J.; Olsen, J. V; Mann, M. In-Gel Digestion for Mass Spectrometric Characterization of Proteins and Proteomes. *Nat. Protoc.* **2006**, *1* (6), 2856–2860. https://doi.org/10.1038/nprot.2006.468.

(42) He, Q.; Huang, Y.; Sheikh, M. S. Proteasome Inhibitor MG132 Upregulates Death Receptor 5 and Cooperates with Apo2L/TRAIL to Induce Apoptosis in Bax-Proficient and -Deficient Cells. *Oncogene* **2004**, *23* (14), 2554–2558. https://doi.org/10.1038/sj.onc.1207351.

(43) Morais, E. R.; Oliveira, K. C.; Paula, R. G. de; Ornelas, A. M. M.; Moreira, É. B. C.; Badoco, F. R.; Magalhães, L. G.; Verjovski-Almeida, S.; Rodrigues, V. Effects of Proteasome Inhibitor MG-132 on the Parasite Schistosoma Mansoni. *PLoS One* **2017**, *12* (9), e0184192. https://doi.org/10.1371/journal.pone.0184192.

(44) Hotez, P.; Ottesen, E.; Fenwick, A.; Molyneux, D. The Neglected Tropical Diseases: The Ancient Afflictions of Stigma and Poverty and the Prospects for Their Control and Elimination. *Adv. Exp. Med. Biol.* **2006**, *582*, 23–33. https://doi.org/10.1007/0-387-33026-7_3.

(45) Adams, J.; Behnke, M.; Chen, S.; Cruickshank, A. A.; Dick, L. R.; Grenier, L.; Klunder, J. M.; Ma, Y. T.; Plamondon, L.; Stein, R. L. Potent and Selective Inhibitors of the Proteasome: Dipeptidyl Boronic Acids. *Bioorganic Med. Chem. Lett.* **1998**, *8* (4), 333–338. https://doi.org/10.1016/S0960-894X(98)00029-8.

(46) Kisselev, A. F.; Goldberg, A. L. Proteasome Inhibitors: From Research Tools to Drug Candidates. *Chem. Biol.* **2001**, *8*, 739–758. https://doi.org/10.1016/S1074-5521(01)00056-4.

(47) Demo, S. D.; Kirk, C. J.; Aujay, M. A.; Buchholz, T. J.; Dajee, M.; Ho, M. N.; Jiang, J.; Laidig, G. J.; Lewis, E. R.; Parlati, F.; Shenk, K. D.; Smyth, M. S.; Sun, C. M.; Vallone, M. K.; Woo, T. M.; Molineaux, C. J.; Bennett, M. K. Antitumor Activity of PR-171, a Novel Irreversible Inhibitor of the Proteasome. *Cancer Res.* **2007**, *67* (13), 6383–6391. https://doi.org/10.1158/0008-5472.CAN-06-4086.

(48) Concannon, C. G.; Koehler, B. F.; Reimertz, C.; Murphy, B. M.; Bonner, C.; Thurow, N.; Ward, M. W.; Villunger, A.; Strasser, A.; Kögel, D.; Prehn, J. H. M. Apoptosis Induced by Proteasome Inhibition in Cancer Cells: Predominant Role of the P53/PUMA Pathway. *Oncogene* **2007**, *26* (12), 1681–1692. https://doi.org/10.1038/sj.onc.1209974.

(49) Imajohohmi, S.; Kawaguchi, T.; Sugiyama, S.; Tanaka, K.; Omura, S.; Kikuchi, H. Lactacystin, a Specific Inhibitor of the Proteasome, Induces Apoptosis in Human Monoblast U937 Cells. *Biochem. Biophys. Res. Commun.* **1995**, *217* (3), 1070–1077. https://doi.org/10.1006/bbrc.1995.2878.

(50) Rojo-Arreola, L.; Long, T.; Asarnow, D.; Suzuki, B. M.; Singh, R.; Caffrey, C. R. Chemical and Genetic Validation of the Statin Drug Target to Treat the Helminth Disease, Schistosomiasis. *PLoS One* **2014**, *9* (1), e87594. https://doi.org/10.1371/journal.pone.0087594.

(51) Kisselev, A. F.; Garcia-Calvo, M.; Overkleeft, H. S.; Peterson, E.; Pennington, M. W.; Ploegh, H. L.; Thornberry, N. A.; Goldberg, A. L. The Caspase-like Sites of Proteasomes, Their Substrate Specificity, New Inhibitors and Substrates, and Allosteric Interactions with the Trypsin-like Sites. *J. Biol. Chem.* **2003**, *278* (38), 35869–35877. https://doi.org/10.1074/jbc.M303725200.

(52) Dick, T. P.; Nussbaum, A. K.; Deeg, M.; Heinemeyer, W.; Groll, M.; Schirle, M.; Keilholz, W.; Stevanović, S.; Wolf, D. H.; Huber, R.; Rammensee, H. G.; Schild, H. Contribution of Proteasomal Beta-Subunits to the Cleavage of Peptide Substrates Analyzed with Yeast Mutants. *J. Biol. Chem.* **1998**, *273* (40), 25637–25646. https://doi.org/10.1074/jbc.273.40.25637.

(53) Giguere, C. J.; Schnellmann, R. G. Limitations of SLLVY-AMC in Calpain and

Proteasome Measurements. *Biochem. Biophys. Res. Commun.* **2008**, *371* (3), 578–581. https://doi.org/10.1016/j.bbrc.2008.04.133.

(54) Wang, Q.; Da'dara, A. A.; Skelly, P. J. The Human Blood Parasite Schistosoma Mansoni Expresses Extracellular Tegumental Calpains That Cleave the Blood Clotting Protein Fibronectin. *Sci. Rep.* **2017**, *7* (1), 1–13. https://doi.org/10.1038/s41598-017-13141-5.

(55) Huber, E. M.; Heinemeyer, W.; Li, X.; Arendt, C. S.; Hochstrasser, M.; Groll, M. A Unified Mechanism for Proteolysis and Autocatalytic Activation in the 20S Proteasome. *Nat. Commun.* **2016**, *7*, 1–10. https://doi.org/10.1038/ncomms10900.

(56) Kisselev, A. F.; Akopian, T. N.; Castillo, V.; Goldberg, A. L. Proteasome Active Sites Allosterically Regulate Each Other, Suggesting a Cyclical Bite-Chew Mechanism for Protein Breakdown. *Mol. Cell* **1999**, *4* (3), 395–402. https://doi.org/10.1016/S1097-2765(00)80341-X.

(57) Li, H.; Ponder, E. L.; Verdoes, M.; Asbjornsdottir, K. H.; Deu, E.; Edgington, L. E.; Lee, J. T.; Kirk, C. J.; Demo, S. D.; Williamson, K. C.; Bogyo, M. Validation of the Proteasome as a Therapeutic Target in Plasmodium Using an Epoxyketone Inhibitor with Parasite-Specific Toxicity. *Chem. Biol.* **2012**, *19* (12), 1535–1545. https://doi.org/10.1016/j.chembiol.2012.09.019.

(58) Li, H.; O'Donoghue, A. J.; van der Linden, W. A.; Xie, S. C.; Yoo, E.; Foe, I. T.; Tilley, L.; Craik, C. S.; da Fonseca, P. C. A.; Bogyo, M. Structure- and Function-Based Design of Plasmodium-Selective Proteasome Inhibitors. *Nature* **2016**, *530* (7589), 233–236. https://doi.org/10.1038/nature16936.

(59) Yoo, E.; Stokes, B. H.; de Jong, H.; Vanaerschot, M.; Kumar, T.; Lawrence, N.; Njoroge, M.; Garcia, A.; Van der Westhuyzen, R.; Momper, J. D.; Ng, C. L.; Fidock, D. A.; Bogyo, M. Defining the Determinants of Specificity of Plasmodium Proteasome Inhibitors. *J. Am. Chem. Soc.* **2018**, *140* (36), 11424–11437. https://doi.org/10.1021/jacs.8b06656.

(60) Kirkman, L. A.; Zhan, W.; Visone, J.; Dziedziech, A.; Singh, P. K.; Fan, H.; Tong, X.; Bruzual, I.; Hara, R.; Kawasaki, M.; Imaeda, T.; Okamoto, R.; Sato, K.; Michino, M.; Alvaro, E. F.; Guiang, L. F.; Sanz, L.; Mota, D. J.; Govindasamy, K.; Wang, R.; Ling, Y.; Tumwebaze, P. K.; Sukenick, G.; Shi, L.; Vendome, J.; Bhanot, P.; Rosenthal, P. J.; Aso, K.; Foley, M. A.; Cooper, R. A.; Kafsack, B.; Doggett, J. S.; Nathan, C. F.; Lin, G. Antimalarial Proteasome Inhibitor Reveals Collateral Sensitivity from Intersubunit Interactions and Fitness Cost of Resistance. *Proc. Natl. Acad. Sci. U. S. A.* **2018**, *115* (29), E6863–E6870. https://doi.org/10.1073/pnas.1806109115.

(61) Nabhan, J. F.; El-Shehabi, F.; Patocka, N.; Ribeiro, P. The 26S Proteasome in Schistosoma Mansoni: Bioinformatics Analysis, Developmental Expression, and RNA Interference (RNAi) Studies. *Exp. Parasitol.* **2007**, *117* (3), 337–347.

(62) Guerra-Sá, R.; Castro-Borges, W.; Evangelista, E. A.; Kettelhut, I. C.; Rodrigues, V. Schistosoma Mansoni: Functional Proteasomes Are Required for Development in the Vertebrate Host. *Exp. Parasitol.* **2005**, *109* (4), 228–236.

https://doi.org/10.1016/j.exppara.2005.01.002.

(63) de Paula, R. G.; Ornelas, A. M. de M.; Morais, E. R.; Borges, W. de C.; Natale, M.; Magalhães, L. G.; Rodrigues, V. Biochemical Characterization and Role of the Proteasome in the Oxidative Stress Response of Adult Schistosoma Mansoni Worms. *Parasitol. Res.* **2014**, *113* (8), 2887–2897. https://doi.org/10.1007/s00436-014-3950-5.

(64) Mathieson, W.; Castro-Borges, W.; Wilson, R. A. The Proteasome-Ubiquitin Pathway in the Schistosoma Mansoni Egg Has Development- and Morphology-Specific Characteristics. *Mol. Biochem. Parasitol.* **2011**, *175* (2), 118–125. https://doi.org/10.1016/j.molbiopara.2010.10.005.

(65) Lindsten, K.; Menéndez-Benito, V.; Masucci, M. G.; Dantuma, N. P. A Transgenic Mouse Model of the Ubiquitin/Proteasome System. *Nat. Biotechnol.* **2003**, *21* (8), 897–902. https://doi.org/10.1038/nbt851.

(66) Kisselev, A. F.; Van Der Linden, W. a.; Overkleeft, H. S. Proteasome Inhibitors: An Expanding Army Attacking a Unique Target. *Chem. Biol.* **2012**, *19* (1), 99–115. https://doi.org/10.1016/j.chembiol.2012.01.003.

(67) Prasad, R.; Atul; Kolla, V. K.; Legac, J.; Singhal, N.; Navale, R.; Rosenthal, P. J.; Sijwali, P. S. Blocking Plasmodium Falciparum Development via Dual Inhibition of Hemoglobin Degradation and the Ubiquitin Proteasome System by MG132. *PLoS One* **2013**, *8* (9), e73530. https://doi.org/10.1371/journal.pone.0073530.

(68) Caffrey, C. R.; Goupil, L.; Rebello, K. M.; Dalton, J. P.; Smith, D. Cysteine Proteases as Digestive Enzymes in Parasitic Helminths. *PLoS Negl. Trop. Dis.* **2018**, *12* (8), e0005840. https://doi.org/10.1371/journal.pntd.0005840.

(69) Kupperman, E.; Lee, E. C.; Cao, Y.; Bannerman, B.; Fitzgerald, M.; Berger, A.; Yu, J.; Yang, Y.; Hales, P.; Bruzzese, F.; Liu, J.; Blank, J.; Garcia, K.; Tsu, C.; Dick, L.; Fleming, P.; Yu, L.; Manfredi, M.; Rolfe, M.; Bolen, J. Evaluation of the Proteasome Inhibitor MLN9708 in Preclinical Models of Human Cancer. *Cancer Res.* **2010**, *70* (5), 1970–1980. https://doi.org/10.1158/0008-5472.CAN-09-2766.

(70) Caffrey, C. R. Chemotherapy of Schistosomiasis: Present and Future. *Curr. Opin. Chem. Biol.* **2007**, *11* (4), 433–439. https://doi.org/10.1016/j.cbpa.2007.05.031.

(71) Olliaro, P.; Seiler, J.; Kuesel, A.; Horton, J.; Clark, J. N.; Don, R.; Keiser, J. Potential Drug Development Candidates for Human Soil-Transmitted Helminthiases. *PLoS Negl. Trop. Dis.* **2011**, *5* (6), 1–8. https://doi.org/10.1371/journal.pntd.0001138.